Titre: Title:	Analyse dynamique des plaques rectangulaires submergées dans un fluide
Auteur: Author:	Erick Charbonneau
Date:	1999
Type:	Mémoire ou thèse / Dissertation or Thesis
Référence: Citation:	Charbonneau, E. (1999). Analyse dynamique des plaques rectangulaires submergées dans un fluide [Mémoire de maîtrise, École Polytechnique de Montréal]. PolyPublie. https://publications.polymtl.ca/8783/

URL de PolyPublie: PolyPublie URL:	https://publications.polymtl.ca/8783/
Directeurs de recherche: Advisors:	
Programme: Program:	Non spécifié

UNIVERSITÉ DE MONTRÉAL

ANALYSE DYNAMIQUE DES PLAQUES RECTANGULAIRES SUBMERGÉES DANS UN FLUIDE

ÉRICK CHARBONNEAU

DÉPARTEMENT DE GÉNIE MÉCANIQUE

ÉCOLE POLYTECHNIQUE DE MONTRÉAL

MÉMOIRE PRÉSENTÉ EN VUE DE L'OBTENTION

DU DIPLÔME DE MAÎTRISE ÈS SCIENCES APPLIQUÉES

(GÉNIE MÉCANIQUE)

DÉCEMBRE 1999

National Library of Canada
Acquisitions and Bibliographic Services
395 Wellington Street
Ottawa ON K1A 0N4
Canada

Bibliothèque nationale du Canada
Acquisitions et services bibliographiques
395, rue Wellington
Ottawa ON K1A 0N4
Canada

Your file Votre référence

Our file Notre référence

0-612-48843-8

Canada

UNIVERSITÉ DE MONTRÉAL

ÉCOLE POLYTECHNIQUE DE MONTRÉAL

Ce mémoire intitulé :

ANALYSE DYNAMIQUE DES PLAQUES RECTANGULAIRES SUBMERGÉES DANS UN FLUIDE

présenté par : CHARBONNEAU Érick

en vue de l'obtention du diplôme de : Maîtrise ès sciences appliquées

a été dûment accepté par le jury d'examen constitué de :

M. PELLETIER Dominique, Ph.D., président

M. LAKIS Aouni A., Ph.D., membre et directeur de recherche

M. SHIRAZI-ADL Aboulfazl, Ph.D., membre

À ma mère et à tous ceux que j'aime...

REMERCIEMENTS

Je tiens à remercier mon directeur de recherche, le professeur M. Aouni A. Lakis, pour le support technique tout au long de ma maîtrise. De plus, je dis un grand merci à Spar Aérospatiale Limitée, maintenant EMS Technologies Canada Limitée, pour leur engagement monétaire et les ressources informatiques fournies lors de cette recherche.

RÉSUMÉ

Ce mémoire présente une méthode permettant de définir les caractéristiques dynamiques d'une plaque isotrope, rectangulaire, mince et élastique dans le vide ou submergé dans un fluide. Il s'agit d'une méthode hybride combinant la théorie des éléments finis avec la théorie classique des plaques minces. Les fonctions de déplacement sont tirées de la solution des équations des plaques et sont développées en série de puissance. L'utilisation de la méthode des éléments finis sur ces fonctions de déplacement permet d'obtenir une matrice de masse et de rigidité pour l'élément de plaque. De plus, ces fonctions de déplacements sont compatibles avec la solution de la pression du fluide à la surface de la plaque.

Le potentiel de vitesse du fluide et l'équation de Bernoulli appliquée à l'interface plaque-fluide permettent d'obtenir une expression de la pression du fluide en fonction des déplacements nodaux de l'élément de plaque et des forces d'inertie du fluide au repos. Une intégration analytique de la pression sur l'élément de fluide conduit à la matrice de masse du fluide.

Les résultats obtenus permettent de conclure que les fréquences calculées par cette méthode sont en accord avec celles obtenues par d'autres auteurs. Par la suite, les effets de différentes conditions aux frontières, de la géométrie de la plaque et de la profondeur du fluide sur les fréquences et modes propres d'une plaque sont étudiés.

ABSTRACT

This thesis presents a method for the dynamic analysis of thin, elastic, isotropic rectangular plate in vacuum or submerged in a fluid. The method is a hybrid of finite element theory and classical thin plate theory. The displacement functions are derived from the solution of the plate differential equation and are expanded in power series. The finite element method applied to these functions leads to the mass and stiffness matrices for the plate element. Moreover, the displacement functions are compatible with the solution of the fluid pressure at the plate surface.

The velocity potential and Bernoulli's equation for a fluid finite element yield an expression for fluid pressure as a function of the nodal displacement of the plate element and inertial force of the fluid at rest. An analytical integration of the fluid pressure over the fluid element leads to the fluid mass matrix.

The results obtained reveal that the frequencies calculated in this way are in good agreement with those obtained by others. The effects of different boundary conditions and plate geometry, together with the depth of submergence, on the dynamic characteristics of rectangular plate were also investigated.

TABLE DES MATIÈRES

LISTE DES TABLEAUX

LISTE DES FIGURES

LISTE DES ANNEXES

INTRODUCTION

Les plaques rectangulaires font partie des éléments structurels les plus couramment utilisées. On les emploie dans différents champs d'application comme l'ingénierie navale et civile, l'aéronautique, et les technologies spatiales. La compréhension des caractéristiques vibratoires des plaques submergées ou non dans un fluide devient donc d'une grande importance et aide les ingénieurs à concevoir de meilleures structures. C'est pour cette raison que le comportement des plaques rectangulaires est, depuis plus de cent ans, le sujet de recherches exhaustives.

Le premier modèle mathématique représentant le comportement d'une membrane fut décrit par Euler au $18^{ième}$ siècle. Plus tard, le physicien allemand Chaldi trouva les premiers modes de vibration d'une plaque horizontale en couvrant de poudre la surface qui vibrait. Cinquante ans plus tard, Lagrange développa la première équation différentielle correcte pour décrire les vibrations d'une plaque libre. Quelques temps après, Navier (1785-1836) introduit une méthode pour calculer les modes et les fréquences propres d'une plaque pour certaines conditions aux frontières. Il utilisa les fonctions trigonométriques découvertes par Fourier pour représenter la déformation d'une plaque.

Kirchoff (1824-1887) est considéré comme le fondateur de la théorie moderne des plaques. En analysant des plaques soumises à de grandes déformations, il comprit

qu'il fallait tenir compte autant l'étirement de la membrane que la flexion lors du calcul de la déformation d'une plaque. Il conclut que les effets non linéaires ne pouvaient être négligés lorsque l'on traite des plaques avec de grandes déformations et que les fréquences naturelles et modes propres peuvent être déterminés par la méthode du travail virtuel. Love (1944) appliqua les travaux de Kirchoff aux plaques épaisses.

Plus récemment, Leissa (1969) a résumé le travail de nombreux chercheurs dans un même ouvrage contenant plus de cinq cents références. L'avènement de l'aviation moderne poussa encore plus loin la recherche dans le domaine des plaques minces. En 1956, Turner et al. (1956) introduisent la méthode des éléments finis qui permettra de résoudre des problèmes de plaques complexes. De plus, avec l'arrivée des ordinateurs, plusieurs méthodes numériques utilisant l'algèbre matricielle seront développées. Zienkiewicz (1977) contribua à la formulation de différentes sortes d'éléments finis. Bogner et al. (1966-1967) travaillèrent sur un élément reposant sur une fonction d'interpolation bi-cubique pour simuler les déplacements d'une plaque.

Dans le but de prédire avec le plus de précision possible autant les basses et hautes fréquences, notre groupe de recherche développa une méthode d'éléments finis hybride qui est basée sur la théorie des coques minces de Sanders (1959). De nombreux éléments ont été développés pour des coques de forme cylindrique, fermée et ouverte, (Lakis et Paidoussis 1971, 1972 et 1973); (Lakis et al. 1978); (Lakis et Sinno 1992), conique (Lakis et al. 1992) et sphérique (Lakis et al. 1989) dans le vide ou contenant un

fluide au repos ou en mouvement. Beaucoup de programmes commerciaux d'éléments finis comme NASTRAN, ABAQUS ou ANSYS peuvent résoudre les problèmes de vibration de plaques dans le vide. Cependant, aucun ne peut prédire correctement les fréquences naturelles d'une plaque submergées dans un fluide. Le but de cette recherche était de trouver un élément fini rectangulaire mince plus général qui pourrait être utilisé ultérieurement pour analyser le système couplé fluide-structure. La formulation de la solution analytique pour un élément de plaque rectangulaire est plutôt complexe : nous avions à trouver des fonctions de déplacement compatibles avec les équations du mouvement de la plaque et, du même coup, compatibles avec la solution d'une plaque en contact avec un fluide. Nous avons donc choisi de transformer la solution homogène de l'équation différentielle bi-harmonique de la plaque rectangulaire en une série de puissance. Ce faisant, nous avons obtenu une solution semi-analytique sous la forme d'un polynôme qui peut être utilisée dans la théorie des éléments finis.

Lamb (1945) fut le premier à décrire la dynamique d'une structure interagissant avec un fluide. Plus tard, Lindholm et al. (1965) conduisit de longues expériences sur la réponse des plaques encastrées submergées dans l'air et l'eau. Leissa (1973) donne plusieurs références sur les réservoirs partiellement remplis de liquide dans son ouvrage dédié aux coques.

D'un autre coté, il ne semble pas y avoir beaucoup d'études sur les structures contenants un liquide avec une surface libre. Récemment, Fu et Price (1987) ont étudié

la réponse des plaques en porte à faux partiellement ou totalement submergées dans un fluide. Ils utilisent une combinaison de la méthode des éléments finis avec une distribution de fonctions de singularité pour examiner l'effet de la surface libre. Robinson et Palmer (1990) développèrent une fonction de pression du fluide en résolvant l'équation d'onde et à l'aide de l'équation de Bernoulli appliquée à l'interface fluide-structure. En utilisant la même philosophie, Soedel et Soedel (1994) donnent une solution analytique pour une plaque simplement supportée supportant un fluide avec une surface libre. Amabili (1996) utilisa la méthode de Rayleigh-Ritz pour obtenir une solution analytique dans le cas où le fluide a une dimension définie par une surface libre ou bien par un mur rigide. L'effet de la profondeur du fluide sur le facteur de masse ajoutée, la fréquence naturelle et les modes propres y sont étudiés. Haddara et Cao (1996) ont adopté la même approche pour analyser de façon analytique et expérimentale la réponse dynamique des plaques rectangulaires submergées avec différentes conditions frontières. Ils obtiennent un facteur de masse ajoutée qui dépend de la hauteur de la surface libre et de la profondeur du fluide en dessous de la plaque.

Comme nous l'avons déjà mentionné, Lakis and Paidoussis (1971) ont étudié les vibrations non forcées d'une coque cylindrique partiellement remplie de liquide en utilisant la méthode des éléments finis avec la théorie classique des coques minces. Dans la même ligne d'idée, Lakis et Neagu (1997) ont analysé l'effet de la surface libre sur la dynamique d'un cylindre à paroi mince partiellement rempli de liquide. Ici,

l'énergie potentielle et cinétique du fluide sont évaluées afin d'établir l'influence de l'oscillation de la surface libre sur la vibration coque-fluide.

Dans le même ordre d'idée, nous présentons dans ce mémoire une méthode pour étudier les caractéristiques dynamiques des plaques rectangulaires minces en contact avec un fluide au repos. Ce mémoire est divisé en deux grandes parties. La première partie, le chapitre 2, traite du développement de l'élément de plaque et de sa précision relative en comparaison avec d'autre théorie. Dans un premier temps, nous déterminons les équations fondamentales de la plaque pour ensuite obtenir les fonctions de déplacement compatible avec la théorie des plaques. Avec ces fonctions de déplacement, nous sommes capables de déterminer les matrices de masse et de rigidité d'un élément finis et, par conséquent, les caractéristiques dynamiques d'une plaque mince vibrant dans le vide.

Au chapitre 3, nous solutionnons l'équation de Laplace pour un potentiel de vitesse avec une surface libre en appliquant l'équation de Bernoulli à l'interface plaque-fluide. Nous obtenons ainsi une expression pour la pression du fluide en fonction des déplacements de la plaques. Une intégration analytique de la pression du fluide sur les éléments de fluide donne la matrice de masse du fluide. Cette dernière est ensuite utilisée avec les matrices de masse et de rigidité de la plaque pour déterminer les effets du fluide sur les fréquences naturelles et modes propres d'une plaque rectangulaire avec différentes conditions aux frontières.

CHAPITRE I

CHAPITRE SYNTHÈSE

Le but premier de cette recherche était de prédire le plus exactement possible les fréquences naturelles d'une plaque rectangulaire submergée dans un fluide. Pour atteindre notre but, il fallait développer un élément fini de plaque rectangulaire dont les fonctions de déplacement sont compatibles avec les équations du mouvement de la théorie des plaques et la solution analytique d'une plaque en contact avec un fluide. De plus, il fallait obtenir un élément fini de fluide défini en fonction des déplacements de la plaque.

Dans un premier temps, le chapitre II présente l'article 1 : *Semi-Analytical Shape Functions in the Finite Element Analysis of Rectangular Plates*. Dans cet article, nous traitons du développement de l'élément de plaque et de sa précision relative en comparaison avec d'autres théories. La formulation de la solution analytique pour un élément de plaque rectangulaire est plutôt complexe. Nous avons donc choisi de transformer la solution générale de l'équation différentielle d'équilibre d'une plaque en flexion en une série de puissance. En faisant cela, nous avons obtenu une solution semi-analytique de la forme d'un polynôme qui peut être utilisée dans la théorie des éléments finis. Il ne restait plus qu'à calculer les matrices de masse et de rigidité de la plaque et à

résoudre le problème aux valeurs propres pour obtenir les fréquences naturelles d'une plaque rectangulaire dans le vide. Les résultats présentés dans l'article 1 auraient pu être calculés en utilisant des méthodes plus rapides que la notre, mais le but principal de cet article est de présenter la méthode et vérifier la véracité de celle-ci.

À la fin de l'article 1, nous validons la méthode pour une plaque vibrant dans le vide en étudiant d'abord la convergence de celle-ci et, puis, en comparant les résultats obtenus avec des résultats expérimentaux et analytiques provenant de divers auteurs. En étudiant la convergence de la méthode, nous avons constaté que celle-ci était rapide compte tenu du fait que la fonction de déplacement utilisée tend à estimer plus exactement la solution d'une plaque en flexion. Grâce à cette fonction de déplacement, il a aussi été démontré que la méthode donne des résultats précis autant pour les basses que les hautes fréquences.

Dans un deuxième temps, le chapitre III introduit, à travers du deuxième article intitulé : *Dynamic Analysis of Rectangular Plates Submerged in Fluids*, la méthode utilisée pour obtenir l'élément fini de fluide. Cet article résume la méthode employée pour résoudre l'équation du potentiel de vitesse avec une surface libre et obtenir l'expression pour la pression du fluide en dessous et au-dessus de la plaque en fonction des déplacements de la celle-ci. Une intégration analytique de la pression sur la surface de la plaque donne la matrice de masse du fluide. Cette matrice de masse est ensuite utilisée avec les matrices de masse et de rigidité de la plaque pour déterminer les effets

du fluide sur les fréquences naturelles et modes propres d'une plaque rectangulaire avec différentes conditions aux frontières. Nous avons prouvé que les variations des fréquences naturelles de la plaque causé par le fluide ne dépendent pas de ses modes propres et très peu des conditions aux frontières. La variation des fréquences naturelles est attribuée à la géométrie de la plaque et aux propriétés du fluide lorsque la première fréquence naturelle du système couplé fluide-structure est supérieure à 10 Hz. De plus, il a été démontré que l'effet du fluide sur le changement des fréquences naturelles devient constant lorsque le fluide atteint une hauteur égale à 40% de la longueur de la plaque. Par contre, lorsque la plaque repose sur une couche mince de fluide, moins de 10% de la longueur de la plaque, les fréquences naturelles de celle-ci tendent vers zéro.

CHAPITRE II

ARTICLE 1[1]

SEMI-ANALYTICAL SHAPE FUNCTIONS IN THE FINITE ELEMENT ANALYSIS OF RECTANGULAR PLATES

E. Charbonneau and **A. A. Lakis**

Department of Mechanical Engineering, École Polytechnique de Montréal, Campus de l'Université de Montréal, C.P. 6079, Succ. Centre-Ville, Montréal, Québec, Canada H3C 3A7

2.1 ABSTRACT

This paper presents a method for the dynamic analysis of a thin, elastic, isotropic rectangular plate. The method is a hybrid of finite element theory and classical thin plate theory. The displacement functions are derived from Sanders' thin-shell equations, and are expanded in power series. Expressions for mass and stiffness are determined by precise analytical integration. The free vibrations of rectangular plates, with various boundary conditions, are studied following this method.

---

[1] Soumis pour publication à Journal of *Sounds and Vibrations*

The results obtained reveal that the frequencies calculated in this manner are in good agreement with those obtained by others.

Keywords: finite element, displacement function, thin plate, vibration

2.2 INTRODUCTION

Rectangular plates are perhaps the most widely used structural elements. They are used in such fields as civil and naval engineering, and in aeronautical and space technology. A knowledge of the free vibration characteristics of rectangular plates enables engineers to design better and lighter structures. For this reason, the behaviour of rectangular plates has been the subject of on-going research for more than a hundred years.

The first mathematical model of the behaviour of the plate membrane was formulated by Euler in the 18th century. Later, the German physicist Chaldi found the vibration modes of horizontal plates by spreading powder on the vibrating surface. More than fifty years later, Lagrange developed the first correct differential equation for the free vibration of plates. Some time later, Navier (1785-1836) produced a method of calculating the mode shape and the frequencies for certain boundary value problems. He used the trigonometric series introduced by Fourier to express the deflection of the plate.

Kirchoff (1824-1887) is considered the founder of modern plate theory which, by analysing plates with substantial deflection, takes into account both the bending and the stretching of the plates. He concluded that the non-linear effects should not be ignored when dealing with large deflections and that the natural frequencies and mode shapes can be determined by the virtual work method. Love[1] applied Kirchoff's work to thick plates.

More recently, Leissa[2] summarized the work of several researchers in a book containing more than five hundred references. The needs of the modern aircraft industry have brought advances in the study of rectangular plates. In 1956, Turner et al.[3] introduced the finite element method, which permits the complex plate problem to be formulated, and, with the advent of high-speed computers, a variety of numerical methods using matrix algebra have been developed. Zienkiewicz[4] contributed to the formulation of different kinds of finite elements. Bogner et al.[5-6] worked on an element using bi-cubic interpolation functions to simulate the displacement of the plate.

In order to predict both low and high frequencies with precision, we used the finite element method with many elements and developed a hybrid finite element method which is derived from Sanders' classical shell theory[7]. Various elements have been developed for close and open cylindrical[8-15], conical[16] and spherical[17] shells in vacuum or containing a fluid at rest or in motion. Whilst several well-known finite element codes such as NASTRAN, ABAQUS or ANSYS can solve the free vibrations of a rectangular plate in vacuum relatively easily, none can correctly predict

the natural frequencies of a plate submerged in fluid. We needed a general, thin, rectangular plate element that could later be used for fluid-structure interaction analysis. The formulation of an analytical solution for a general rectangular plate element is quite complex: we had to find displacement functions compatible with both the plate equations of motion and the solution of a plate in contact with fluid. We decided, therefore, to expand the homogenous solution of the bi-harmonic equation of plate into a power series and, in so doing, we obtained a semi-analytical solution in the form of a polynomial which can be used in classical finite element theory.

In this article, we discuss the development of this element and its relative accuracy in comparison with other methods. We first determined the fundamental equations of the plate and, secondly, derived the displacement functions of plate theory and expanded them in power series. With these displacement functions, we were able to determine the mass and stiffness matrices required by the finite element method and, therefore, the free vibration characteristics of the plate.

2.3 FUNDAMENTAL EQUATIONS FOR A THIN RECTANGULAR PLATE

2.3.1 Equilibrium equations

To establish the equilibrium equations of the plate, we use Sanders' equations [7] for cylindrical shells and assume the radius to be infinite, $\theta = y$ and $rd\theta = dy$. These three equations take into account both membrane and bending effects. Sanders based

his equations on Love's first approximation [1] for thin shells, and showed that all strains vanish for any rigid-body motion. For the finite element method this theory satisfies the convergence criteria for small rigid-body motions.

The geometry of the mean surface and the co-ordinate system used for this analysis are shown in figure 2.1.

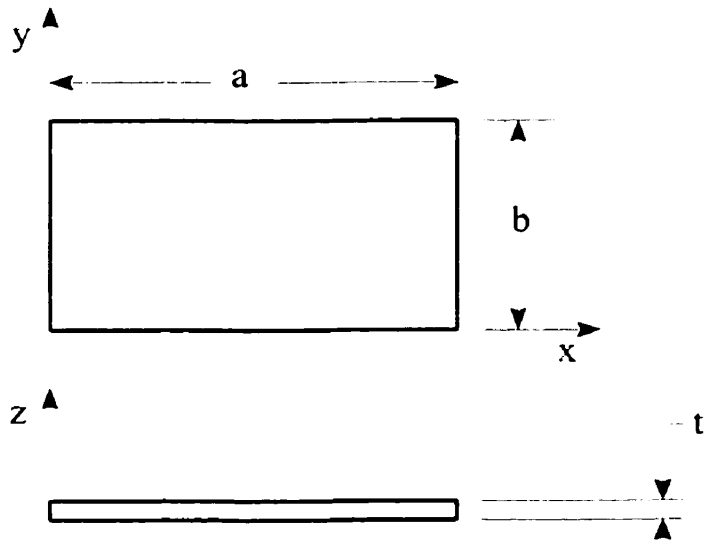

Fig. 2.1. Geometry of rectangular plate's mean surface

The equilibrium equations for a rectangular plate, following Sanders' theory, are written as follows:

$$\frac{\partial \overline{N}_{x}}{\partial x} + \frac{\partial N_{xy}}{\partial y} = 0$$

$$\frac{\partial N_{xx}}{\partial x} + \frac{\partial N_{xy}}{\partial y} = 0 \qquad (2.1)$$

$$\frac{\partial^2 M_{xx}}{\partial x^2} + 2\frac{\partial^2 M_{xy}}{\partial x \partial y} + \frac{\partial^2 M_{yy}}{\partial y^2} = 0$$

where N_{xx}, N_{xy}, N_{yy}, M_{yy}, M_{xx} and M_{xy} are the stress components per unit length and x and y are the coordinates of the plate. The unit vectors corresponding to the stresses defined in Equation (2.1) are indicated on Figure 2.2.

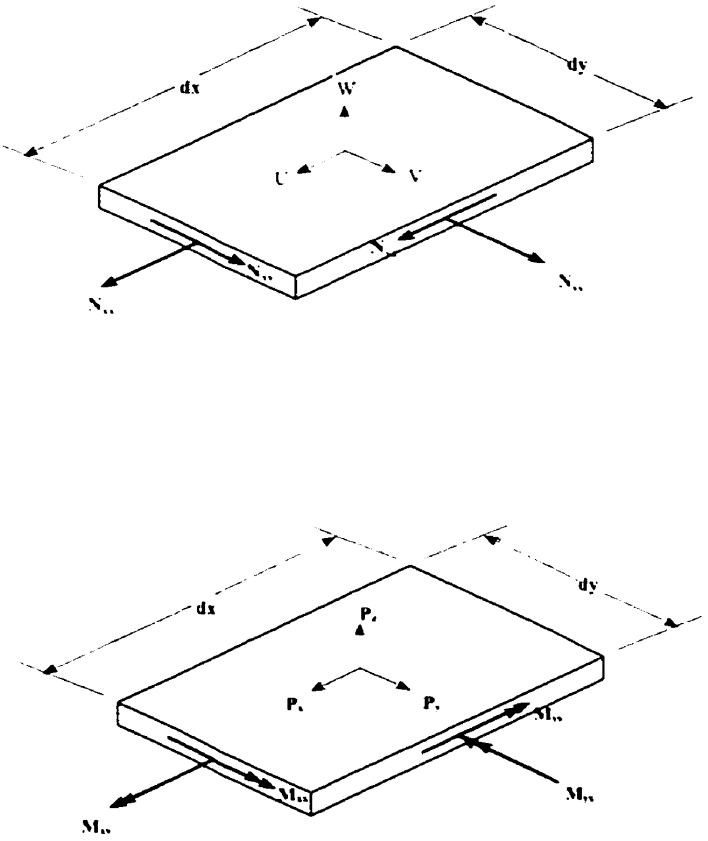

Fig. 2.2. Differential element for a rectangular plate

2.3.2 Kinematics equations

The relation between the strain (ε) and the displacement for a rectangular plate is given as follows:

$$\begin{pmatrix} \varepsilon_x \\ \varepsilon_y \\ 2\varepsilon_{xy} \\ \kappa_x \\ \kappa_y \\ \kappa_{xy} \end{pmatrix} = \begin{Bmatrix} \dfrac{\partial U}{\partial x} \\ \dfrac{\partial V}{\partial y} \\ \dfrac{\partial V}{\partial x} + \dfrac{\partial U}{\partial y} \\ -\dfrac{\partial^2 W}{\partial x^2} \\ -\dfrac{\partial^2 W}{\partial y^2} \\ -\dfrac{\partial^2 W}{\partial x \partial y} \end{Bmatrix} \tag{2.2}$$

where U and V are the in plane displacements and W the deflection of the plate.

For an anisotropic and elastic material the relationship between stress and strain is

$$\{\sigma\} = [P]\{\varepsilon\} \tag{2.3}$$

where [P] is a 6x6 symmetric elasticity matrix. In the case of an isotropic material there is no coupling between membrane and bending effects, and the only non-vanishing terms are:

$$P_{11} = P_{22} = D \quad P_{44} = P_{55} = K$$

$$P_{12} = P_{21} = \nu D \quad P_{45} = P_{54} = \nu K \tag{2.4}$$

$$P_{33} = \frac{(1-\nu)}{2} D \quad P_{66} = \frac{(1-\nu)}{2} K$$

where D and K are respectively the membrane and bending stiffness defined as

$$D = \frac{Et}{1-\nu^2} \qquad K = \frac{Et^3}{12(1-\nu^2)}$$

E being the young's modulus, ν the Poisson's ratio and t the plate thickness.

Next, we substitute Equations (2.2) and (2.3) in the equilibrium equations to obtain the 3 equations of motion in terms of the in-plane and normal displacements of the plate's mean surface (U, V, W).

$$P_{22}\frac{\partial^2 V}{\partial y^2} + P_{21}\frac{\partial^2 U}{\partial x \partial y} + P_{33}\left(\frac{\partial^2 U}{\partial x \partial y} + \frac{\partial^2 V}{\partial x^2}\right) = 0$$

$$P_{11}\frac{\partial^2 U}{\partial x^2} + P_{12}\frac{\partial^2 V}{\partial x \partial y} + P_{33}\left(\frac{\partial^2 V}{\partial x \partial y} + \frac{\partial^2 U}{\partial y^2}\right) = 0 \tag{2.5}$$

$$P_{44}\frac{\partial^4 W}{\partial x^4} + \frac{\partial^4 W}{\partial x^2 \partial y^2}(P_{45} + P_{54} + 2P_{66}) + P_{55}\frac{\partial^4 W}{\partial y^4} = 0$$

The first two equations in (2.5) describe the membrane behavior and the last equation defines the bending of a rectangular plate. By solving these equations, it is possible to find the displacement function in terms of the nodal displacements.

2.4 DISPLACEMENT FUNCTIONS

2.4.1 Solution of the differential equations

In this instance, we are dealing with the case of isotropic material. As can be seen in Equation (2.5), the equations of motion are decoupled. It is possible, therefore, to consider the membrane and bending equations to be two different problems, each with its own solution.

The solution for the membrane differential equations in Equation (5) is based on Szilard [20]. We assume the solution to be a bi-linear polynomial expressing the nodal displacements in U and V, where U and V are, respectively, the in-plane displacement in the x and y direction as can be shown on an element in Figure 2.3.

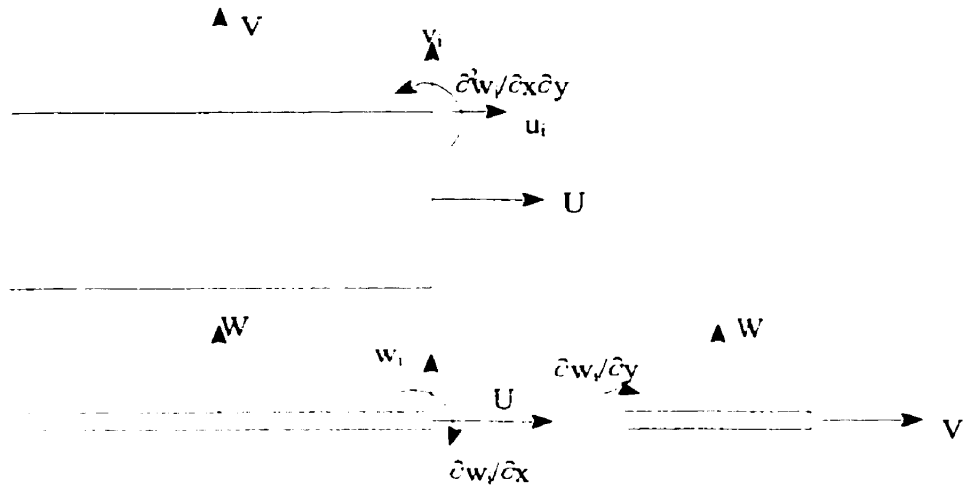

Fig. 2.3. Displacements and degrees of freedom of a rectangular plate

The polynomial expression will be as follows:

$$U(x,y) = C_1 + C_2\frac{x}{a} + C_3\frac{y}{b} + C_4\frac{xy}{ab}$$

$$V(x,y) = C_5 + C_6\frac{x}{a} + C_7\frac{y}{b} + C_8\frac{xy}{ab} \qquad (2.6)$$

where x and y and the element coordinate system and a and b are the lenght and width of the plate corresponding to the x and y coordinates. These assumed displacement functions contain the same number of unknown parameters C_i as the number of nodal displacements (2 x 4 = 8). The solution is rather crude but converges monotonically almost to the "exact" value for the problem of finding the maximum deflection[20].

In the case of bending, the bi-harmonic equation has a general solution of the following form:

$$W(x,y) = \sum_{i=1}^{n} C_i e^{\frac{x}{a}+\frac{y}{b}} \qquad (2.7)$$

where W is the normal deflection of the plate element shown in figure 2.3. Since it is a complex matter to find the characteristic equation, we expand the solution in a Taylor series. The number of terms in the series remains to be determined. Furthermore, the number of degrees of freedom describing the motion of the plate in its normal direction is governed by the number of terms in the series. Therefore, we add as many terms as the hermitian bi-cubic polynomial used by Bogner[6]. The expanded polynomial, which approximates the normal deflection of the element, is:

$$W_p(x,y) = \left[\sum_{i=0}^{3} \frac{A_i}{i!}\left(\frac{x}{a}\right)^i\right]\left[\sum_{j=0}^{3} \frac{B_j}{j!}\left(\frac{y}{b}\right)^j\right] \tag{2.8}$$

where i! means i factorial; i.e., for i = 3, i! = 1x2x3. Equation (2.8) gives 16 unknown parameters A_i and B_j corresponding, again, to the number of degrees of freedom per element for bending. Figure 2.3 shows the nodal degrees of freedom (W, $\partial W/\partial x$, $\partial W/\partial y$, $\partial^2 W/\partial x \partial y$) which relate to the bending motion. Instead of a rotational degree of freedom about the z-axis, we have the second derivative of W, which gives the twisting strain, and ensures a continuity of slope between the elements. This gives conforming and compatible elements in bending.

Furthermore, when using a power series to express the displacement function, we approach the "exact" solution of the bending equation more closely than Bogner et al. [5-6] did with the bi-cubic polynomial. The two displacement functions are compared to the exact Equation (2.7) in Figure 2.4.

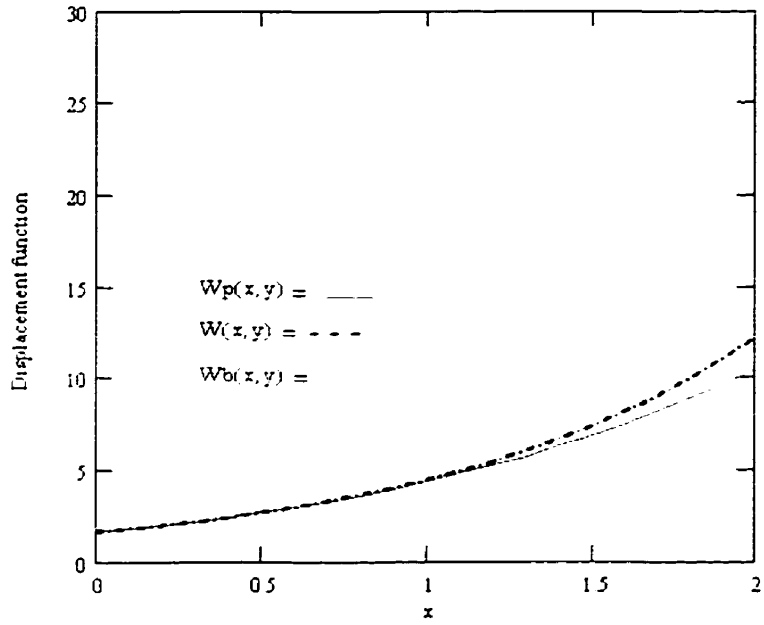

Fig. 2.4. Comparison of displacement functions: equation (2.8) $W_p(x,y)$: ——— ; Bogner[6] $W_b(x,y)$: — — ; and the exact solution equation (2.7) $W(x,y)$: – . –

2.4.2 Displacement functions for a finite element

We can write the displacement U,V and W in matrix form:

$$\begin{Bmatrix} U \\ V \\ W \end{Bmatrix} = [R] \quad \{C\} \tag{2.9}$$

where [R] is a 3x24 matrix in which the components are the x and y terms of Equations (2.6) and (2.8) without the unknown constants. The vector {C} is given by:

$$\{C\} = \{C_1, \ldots, C_{24}\}^t \tag{2.10}$$

To determine these constants, we need to define twenty-four conditions for the finite element. These twenty-four conditions will be the twenty-four degrees of freedom of the element, which means six degrees of freedom per node as follows:

$$\{\delta_1, \delta_2, \delta_3, \delta_4\}^t = \{u_1, v_1, w_1, w_{1,x}, w_{1,y}| w_{1,xy}, u_2, v_2, w_2, w_{2,x}, w_{2,y}, w_{2,xy}|u_3, v_3, w_3, w_{3,x}, w_{3,y}, w_{3,xy}| u_4, v_4, w_4, w_{4,x}, w_{4,y}, w_{4,xy}\} \quad (2.11)$$

where the δ_is are the generalized nodal displacement and $w_{i,x}$ is the derivative of w_i respect to x and so on. Then, we have to define a transformation matrix [A] to relate the displacement functions $\{C_i\}$ and the nodal displacements $\{\delta_i\}$:

$$\{\delta_i\} = [A]\{C_i\} \quad (2.12)$$

[A] is a 24x24 matrix listed in Appendix I. The terms of matrix [A] are obtained from matrix [R] by going from node 1 to node 4 and setting the value of x to 0 or a, and of y to 0 or b. By multiplying Equation (12) by $[A]^{-1}$ and substituting into equation (2.9) we obtain

$$\begin{Bmatrix} U \\ V \\ W \end{Bmatrix} = [R] \quad [A]^{-1} \begin{Bmatrix} \delta_1 \\ \delta_2 \\ \delta_3 \\ \delta_4 \end{Bmatrix} = [N] \begin{Bmatrix} \delta_1 \\ \delta_2 \\ \delta_3 \\ \delta_4 \end{Bmatrix} \quad (2.13)$$

where [N] is the displacement function matrix for a finite element of rectangular plate.

2.5 STRESS AND STRAIN VECTORS

The strain vector can be found by using equations (2.2) and (2.13):

$$\{\varepsilon\} = [D] \quad [R] \quad [A^{-1}] \quad \begin{Bmatrix} \delta_1 \\ \delta_2 \\ \delta_3 \\ \delta_4 \end{Bmatrix} = [B] \quad \begin{Bmatrix} \delta_1 \\ \delta_2 \\ \delta_3 \\ \delta_4 \end{Bmatrix} \tag{2.14}$$

where [D] is a matrix containing the derivative operators from equation (2.2). After defining the strain vector, we can use it and refer to equation (2.3) for the stress vector:

$$\{\sigma\} = [P] \quad \{\varepsilon\} = [P] \quad [B] \quad \begin{Bmatrix} \delta_1 \\ \delta_2 \\ \delta_3 \\ \delta_4 \end{Bmatrix} \tag{2.15}$$

2.6 MASS AND STIFFNESS MATRICES FOR ONE FINITE ELEMENT

Using the finite element theory[4], the mass and stiffness matrices may be expressed as:

$$[m] = \rho \quad t \int_0^a \int_0^b [N]^T \quad [N] \quad dA$$

(2.16)

$$[k] = \int_0^a \int_0^b [B]^T [P] \quad [B] \quad dA$$

(2.17)

where dA= dy dx. The matrices [N], [P] and [B] are given in equations (2.13) (2.14) and (2.3). Integrating equations (2.16) and (2.17) over x and y, we obtain:

$$[m] = [A^{-1}] [S] [A^{-1}]$$

(2.18)

$$[k] = [A^{-1}] [G] [A^{-1}]$$

(2.19)

where [S] and [G] are 24x24 real symmetrical matrices. For the mass matrix, [S] is partionned as follows:

$$[S] = \begin{bmatrix} S^{(u)}_{4x4} & \vdots & 0 & \vdots & 0 \\ \cdots & \vdots & \cdots & \vdots & \cdots \\ 0 & \vdots & S^{(v)}_{4x4} & \vdots & 0 \\ \cdots & \vdots & \cdots & \vdots & \cdots \\ 0 & \vdots & 0 & \vdots & S^{(w)}_{16x16} \end{bmatrix} \qquad (2.20)$$

The elements of the symmetrical submatrices are given by

$$S_{ij}^{(u)} = S_{ij}^{(v)} = A_{ij}\ a\ b$$

(2.21)

$$S_{ij}^{(w)} = B_{ij}\ a\ b$$

where the constants A_{ij} and Bi_j are found in Table 2.1.

In the case of the stiffness matrix, [G] is partitioned as follows:

$$[G]=\begin{bmatrix} G^{(u)}{}_{4\times4} & \vdots & G^{(uv)}{}_{4\times4} & \vdots & 0 \\ \cdots & \vdots & \cdots & \vdots & \cdots \\ G^{(vu)}{}_{4\times4} & \vdots & G^{(v)}{}_{4\times4} & \vdots & 0 \\ \cdots & \vdots & \cdots & \vdots & \cdots \\ 0 & \vdots & 0 & \vdots & G^{(w)}{}_{16\times16} \end{bmatrix} \tag{2.22}$$

We can see from this matrix that a rectangular plate element has a coupling between u and v in the membrane part and no coupling between membrane and bending for an isotropic material. The elements of the submatrices are given by the Equation (2.23), where the constants $E_{ij}^{(k)}$, k=1, 2, ..., 8, and the exponents L_{ij}, M_{ij} are given in Table 2.1.

$$G_{ij}^{(u)} = \frac{D}{ab}\left(E_{ij}^{(1)}b^2 + (1-\nu)a^2E_{ij}^{(2)}\right) \qquad G_{ij}^{(uv)} = D\left(E_{ij}^{(3)}\nu + (1-\nu)E_{ij}^{(4)}\right)$$

$$G_{ij}^{(v)} = \frac{D}{ab}\left(E_{ij}^{(2)}b^2 + (1-\nu)a^2E_{ij}^{(1)}\right) \qquad G_{ij}^{(vu)} = D\left(E_{ij}^{(4)}\nu + (1-\nu)E_{ij}^{(3)}\right) \tag{2.23}$$

$$G_{ij}^{(w)} = \frac{K}{ab}\left(E_{ij}^{(5)}\left(\frac{a}{b}\right)^{L_{ij}} + E_{ij}^{(6)}\frac{(1-\nu)}{2} + E_{ij}^{(7)}\nu + E_{ij}^{(8)}\left(\frac{b}{a}\right)^{M_{ij}}\right)$$

Table 2.1 Constants and exponents for symmetric submatrices

i	j	A_{ij}	B_{ij}	$E_{ij}^{(1)}$	$E_{ij}^{(2)}$	$E_{ij}^{(3)}$	$E_{ij}^{(4)}$	$E_{ij}^{(5)}$	$E_{ij}^{(6)}$	$E_{ij}^{(7)}$	$E_{ij}^{(8)}$	L_{ij}	M_{ij}	i	j	B_{ij}	$E_{ij}^{(5)}$	$E_{ij}^{(6)}$	$E_{ij}^{(7)}$	$E_{ij}^{(8)}$	L_{ij}	M_{ij}
1	1	1.9	1.63504	1.3	1.3	1.4	1.4	1.756	1.460	1.450	1.756	2	2	5	15	1.180	0	0	0	0		
1	2	1.6	1.18144	1.1	0	0	1.2	1.504	1.160	1.180	1.216	2	2	5	16	1.144	0	0	0	0		
1	3	1.6	1.7560	0	1.1	1.2	0	0	1.120	1.8	1.90	0	0	6	6	1.460	1.20	1.9	1.18	1.20	2	2
1	4	1	1.6048	0	0	0	0	0	0	1.60	1.72	0	2	6	7	1.160	0	1.6	1.12	1.8	0	2
1	5	1	1.18144					1.216	1.160	1.180	1.504	2	2	6	8	1.120	0	0	0	1.6	0	2
1	6	1	1.5184					1.144	1.64	1.96	1.144	2	2	6	9	1.576	1.16	1.16	1.16	0	2	
1	7	1	1.2160					0	1.48	1.72	1.60	0	2	6	10	1.160	1.8	1.6	1.12	0	2	
1	8	1	1.1728					0	0	1.48	1.48	0	2	6	11	1.64	0	1.4	0	0		
1	9	1	1.7560					1.90	1.120	1.90	0	2		6	12	1.48	0	0	0	0		
1	10	1	1.2160					1.60	1.48	1.72	0	2		6	13	1.432	1.12	0	1.8	0	2	
1	11	1	1.960					0	1.36	0	0			6	14	1.120	1.6	0	1.6	0	2	
1	12	1	1.720					0	0	0	0			6	15	1.48	0	0	0	0		
1	13	1	1.6048					1.72	0	1.60	0	2		6	16	1.36	0	0	0	0		
1	14	1	1.1728					1.48	0	1.48	0	2		7	7	1.60	0	1.3	0	1.3		2
1	15	1	1.720					0	0	0	0			7	8	1.46	0	0	0	1.2		2
1	16	1	1.576					0	0	0	0			7	9	1.240	0	1.12	1.6	0		
2	2	1.3	1.5040	1	0	0	0	1.252	1.60	1.90	1.60	2	2	7	10	1.64	0	1.4	1.4	0		
2	3	1.1	1.2016	0	0	1	0	0	1.40	1.60	1.20	0	2	7	11	1.24	0	1.2	0	0		
2	4	1.2	1.1512	0	0	0	0	0	0	1.30	1.18	0	2	7	12	1.16	0	0	0	0		
2	5		1.5184					1.144	1.96	10.576	1.144	2	2	7	13	1.180	0	0	1.3	0		
2	6		1.1440					1.72	1.24	1.36	1.40	2	2	7	14	1.48	0	0	1.2	0		
2	7		1.576					0	1.16	1.48	1.16	2	2	7	15	1.18	0	0	0	0		
2	8		1.432					0	0	1.24	1.12	2	2	7	16	1.12	0	0	0	0		
2	9		1.2160					1.60	1.48	1.24	0	2		8	8	1.20	0	0	0	1		2
2	10		1.960					1.30	1.18	1.18	0	2		8	9	1.192	0	0	1.4	0		
2	11		1.240					0	1.12	0	0			8	10	1.48	0	0	1.2	0		
2	12		1.180					0	0	0	0			8	11	1.16	0	0	0	0		
2	13		1.1728					1.48	0	1.16	0	2		8	12	1.8	0	0	0	0		
2	14		1.480					1.24	0	1.12	0	2		8	13	1.144	0	0	1.2	0		
2	15		1.192					0	0	0	0			8	14	1.136	0	0	1	0		
2	16		1.144					0	0	0	0			8	15	1.12	0	0	0	0		
3	3	1.3	1.756	0	1	0	0	0	1.20	0	1.9		2	8	16	1.6	0	0	0	0		
3	4	1.1	1.504	0	0	0	0	0	0	0	1.6		2	9	9	1.756	1.9	1.20	0	0	2	
3	5		1.2160					0	1.48	1.24	1.60		2	9	10	1.216	1.6	1.8	0	0	2	
3	6		1.576					0	1.16	1.16	1.16		2	9	11	1.90	0	1.6	0	0		
3	7		1.216					0	1.8	0	1.6		2	9	12	1.72	0	0	0	0		
3	8		1.144					0	0	1.4	1.4		2	9	13	1.504	1.6	0	0	0	2	
3	9		1.960					0	1.36	1.9	0			9	14	1.144	1.4	0	0	0	2	
3	10		1.240					0	1.12	1.6	0			9	15	1.60	0	0	0	0		
3	11		1.60					0	1.0	0	0			9	16	1.48	0	0	0	0		
3	12		1.60					0	0	0	0			10	10	1.60	1.4	1.4	0	0	2	
3	13		1.720					0	0	1.6	0			10	11	1.24	0	1.2	0	0	2	
3	14		1.192					0	0	1.4	0			10	12	1.18	0	0	0	0		
3	15		1.72					0	0	0	0			10	13	1.144	1.4	0	0	0	2	
3	16		1.48					0	0	0	0			10	14	1.40	1.2	0	0	0	2	
4	4	1	1.252	0	0	0	0	0	0	0	1.3		2	10	15	1.16	0	0	0	0		
4	5		1.1728					0	0	1.16	1.48		2	10	16	1.12	0	0	0	0		
4	6		1.432					0	0	1.8	1.12		2	11	11	1.9	0	0	0	0		
4	7		1.144					0	0	0	1.4		2	11	12	1.6	0	0	0	0		
4	8		1.72					0	0	0	1.2		2	11	13	1.60	0	0	0	0		
4	9		1.720					0	0	1.6	0			11	14	1.16	0	0	0	0		
4	10		1.180					0	0	1.3	0			11	15	1.6	0	0	0	0		
4	11		1.60					0	0	0	0			11	16	1.4	0	0	0	0		
4	12		1.30					0	0	0	0			12	12	1.3	0	0	0	0		
4	13		1.576					0	0	1.4	0			12	13	1.48	0	0	0	0		
4	14		1.144					0	0	1.2	0			12	14	1.12	0	0	0	0		
4	15		1.48					0	0	0	0			12	15	1.4	0	0	0	0		
4	16		1.24					0	0	0	0			12	16	1.1	0	0	0	0		
5	5		1.5040					1.60	1.60	1.252	1.90	2	2	13	13	1.252	1.3	0	0	0	2	
5	6		1.1440					1.40	1.24	1.36	1.72	2	2	13	14	1.72	1.2	0	0	0	2	
5	7		1.600					0	1.18	1.18	1.30		2	13	15	1.30	0	0	0	0		
5	8		1.480					0	0	1.12	1.24		2	13	16	1.24	0	0	0	0		
5	9		1.2016					1.20	1.40	1.60	0	2		14	14	1.20	1	0	0	0	2	
5	10		1.576					1.16	1.16	1.48	0	2		14	15	1.8	0	0	0	0		
5	11		1.240					0	1.12	0	0			14	16	1.6	0	0	0	0		
5	12		1.192					0	0	0	0			15	15	1.3	0	0	0	0		
5	13		1.1512					1.18	0	1.30	0	2		15	16	1.2	0	0	0	0		
5	14		1.432					1.12	0	1.24	0	2		16	16	1	0	0	0	0		

2.7 CALCULATION AND DISCUSSION

2.7.1 Free vibrations

The complete plate is subdivided into finite elements, each of which is a smaller rectangular plate. The position of the nodal points are chosen in such a way that the local coordinate system of the element is parallel with the global coordinate system of the plate.

Once the stiffness and the mass matrices have been obtained it is possible to construct the global matrices for the complete plate using finite element assembly technique. If N is the number of nodes then [M] and [K] are two matrices of order 6N. In the case of free vibration, the equations of motion are:

$$[M]\left\{\ddot{\delta}_T\right\} + [K]\left\{\delta_T\right\} = \{0\} \tag{2.24}$$

where $\{\delta\}_T$ is the vector for global displacements of the whole shell.

$$\{\delta_T\} = \{\delta_1, \delta_2, \ldots, \delta_N\}^t \tag{2.25}$$

N being the number of nodes. By specifying

$$\{\delta_T\} = \{\delta_{0,T}\} \sin(\omega t + \phi) \tag{2.26}$$

where ω is natural angular frequency and ϕ is the phase angle.

By introducing equation (2.24) and (2.25), we obtain the typical eigenvalue and eigenvector problem:

$$\det [[K] - \omega^2 [M]] = 0 \tag{2.27}$$

We have proven in earlier sections that the stretching equations are decoupled from the bending equations. For this reason, the solution of equation (2.27) gives us both the bending and in plane modes. The shape of the eigenvector for each mode will permit us to differentiate the bending modes from the in plane modes.

2.7.2 Convergence

The accuracy of the finite element method depends on the number of elements used to discretize the physical problem. A preliminary set of calculations was undertaken to determine the requisite number of finite elements for an accurate determination of the natural frequencies. Calculations were made with a rectangular steel plate having the following properties: a =609.6 mm, b = 304.8 mm, t = 2.54 mm, E = 196×10^9 N/m^2, $\nu = 0.3$, $\rho = 7.86$ kg/m^3 and with the number of elements N = 1, 2, 4, 8, 16, 32, 64. The boundary conditions correspond to a simply supported plate on all edges. The results for the first 6 natural frequencies are given in Figure 2.5. We conclude that the convergence of the system is fast. About eight elements are needed for convergence. For convergence at higher frequencies, more elements must be used. The reason for this is simple: since we are using polynomials to represent the mode shapes,

we need more degrees of freedom, and hence a greater number of elements, to have a satisfactory representation of the higher mode shapes.

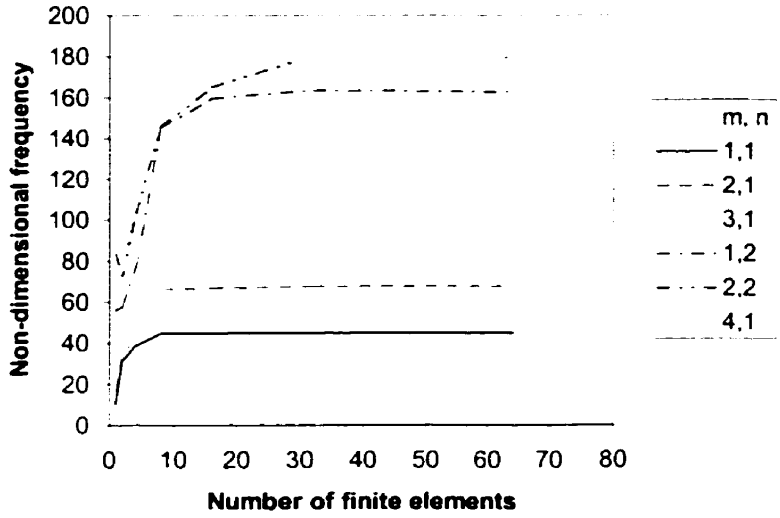

Fig. 2.5. Non-dimensional natural frequency, $\Omega = \omega a^2(\rho t/K)^{1/2}$, of a simply supported rectangular plates as a function of the number of finite elements for the first six modes.

2.7.3 Calculations for rectangular plates

The eigenvalues of a uniform rectangular plate with different boundary conditions may be calculated in a simpler way. In fact, Leissa[2] gives a good summary and all the tables needed to solve the kind of problems discussed here. Our main aim is to test the correctness of the mass and stiffness matrices as developed in this paper.

We first determine the natural frequencies of the rectangular plate and compare them to the exact solution. This comparison enables us to give the relative precision of

the method for 64 elements. Figure 2.6 gives the first six mode shapes and natural frequencies computed. By looking at the deformed shape, we can tell the number of axial modes in both directions where m is the longest side (x axis) and n is the shortest side (y axis). The error between the finite element model and the exact solution is given in Table 2.2.

Table 2.2. Relative error between the exact solution of rectangular plate simply supported and a 64 finite element model.

m, n	1, 1	2, 1	3, 1	1, 2	2, 2	4, 1
Exact solution ; f (Hz)	83.50	133.61	217.12	283.9	334.0	334.0
Our method ; f (Hz)	76.16	114.69	191.27	275.44	303.94	305.19
% error	**8.79**	**14.16**	**11.91**	**2.98**	**9.00**	**8.63**

Table 2.2 shows fairly good result for the finite element method as compared with the exact solution. The error varies from 3 to 15 percent depending on the mode.

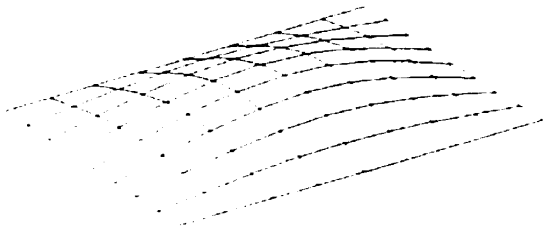

a) $f_{1,1}$ = 76.16 Hz

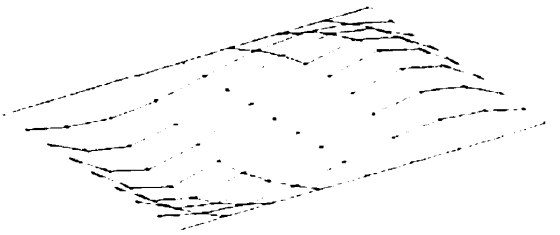

b) $f_{2,1}$ = 114.69 Hz

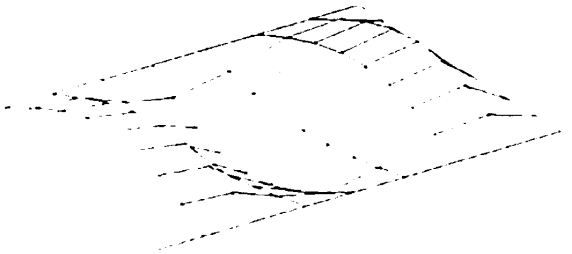

c) $f_{3,1}$ = 191.27 Hz

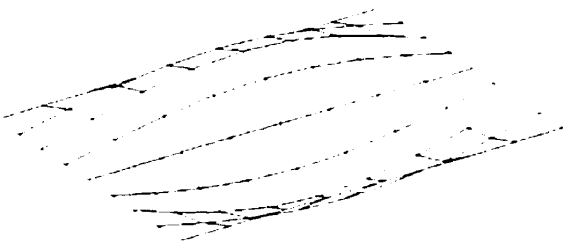

d) $f_{1,2}$ = 275.44 Hz

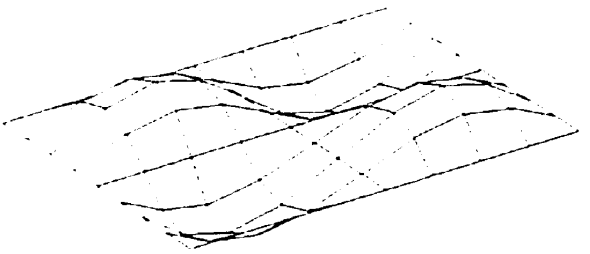

d) $f_{2,2}$ = 303.94 Hz

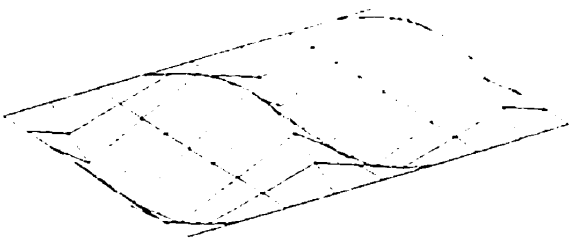

e) $f_{4,1}$ = 305.19 Hz

Fig. 2.6. Computed mode shapes of the simply supported plate

We performed a second set of calculations to compare our method with experimental values and other numerical methods. The calculations were carried out using two different boundary conditions: a) clamped on the shortest side and the three other edges free, b) simply supported on two opposite edges and the two other edges free. As there is no exact solution to the problem of the cantilevered plate, we verified the performance of our method against that of other numerical solutions. A solution was also obtained by Martin[18], who used a variational procedure similar to the Rayleigh-Ritz method for a cantilevered rectangular steel plate of dimensions: a = 5.12 in, b = 2.76 in and t = 0.053 in. Our results are shown in Table 2.3 and compared to those of Martin[18] and to the experimental data of Grinsted[19]. Figure 2.7 shows the associated eigenvectors.

Table 2.3. Comparison of a cantilever rectangular steel plate natural frequencies

n	*Type*	*Frequency in Hz, for values of m of:*		
		1	2	3
1	Theoretical[18]	69.5	436	1220
	Experimental[19]	64	405	1120
	Our method	67.58	420.62	1170.41
3	Theoretical[18]	1610	2260	
	Experimental[19]	1606	nd	
	Our method	1532.91	1798.72	

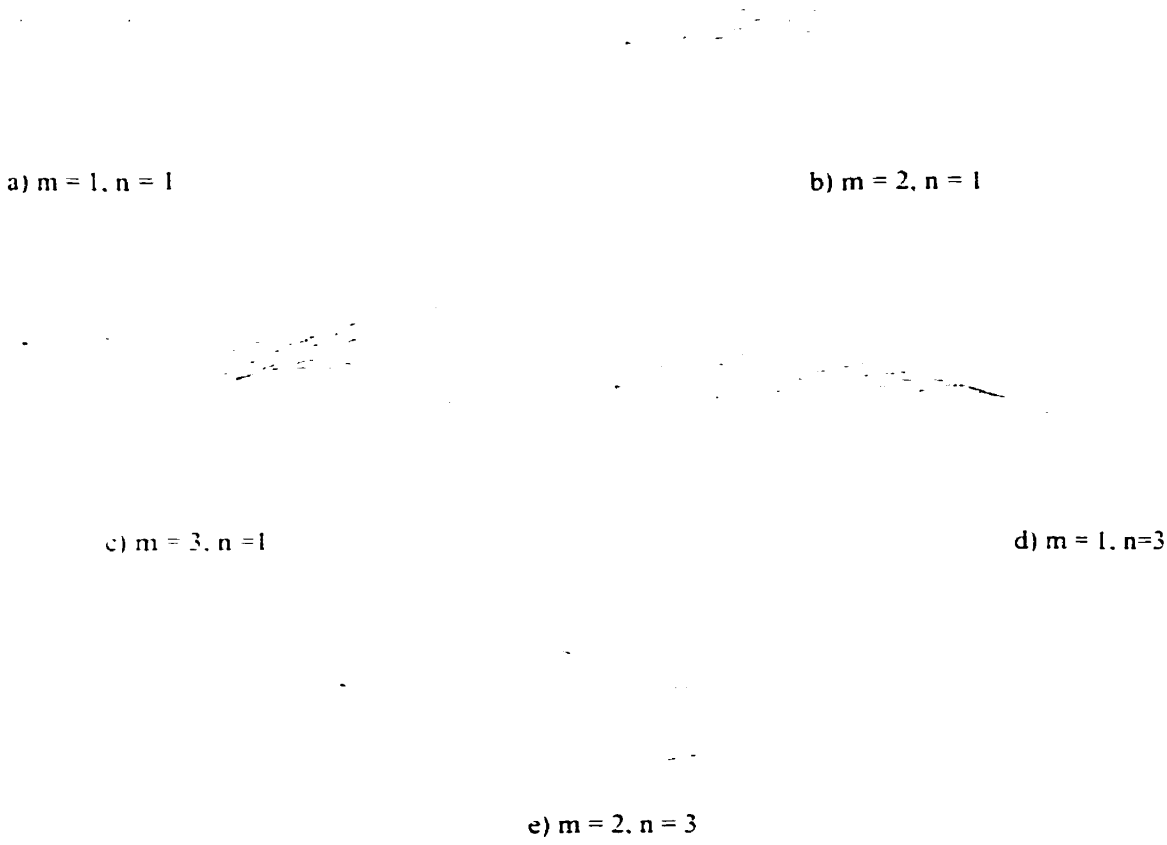

Fig. 2.7. Computed mode shapes of the cantilever plate

We calculated the natural frequencies of the cantilevered plate using an 8x8-element model. As may be seen, the results obtained by this method are in satisfactory agreement with those obtained using the other theory and with the experimental results. The natural frequencies and mode shapes of the rectangular steel plate simply supported on the two shortest opposite sides were also calculated. Since there is an analytical and an "exact" solution to the problem, the analysis increases our confidence in the

calculation of the symmetrical model. To do this, we analysed a steel plate which has the following dimensions: a = 609.6 mm, b = 304.8 mm and t = 2.54 mm. The results obtained by our method were calculated using an 8x8 element model and are compared to the analytical solution in Table 2.4.

Table 2.4. Natural frequencies, in Hz, for a rectangular steel plate simply supported on opposite edges calculated numerically and analytically.

m, n	1, 1	2, 1	3, 1	1, 3
Analytical solution	16.7	66.8	150.3	178.5
Our method	15.98	64.37	145.86	161.30
% error	**4.31**	**3.64**	**2.95**	**9.636**

As can be seen, all the modes are computed with a relatively good accuracy.

2.8 CONCLUSION

The objective of this paper was to present a new method for deriving the displacement functions of a thin rectangular plate and, subsequently, to use these displacement function in dynamic analysis and fluid-structure interaction. The mass and stiffness matrices of a twenty-four degrees of freedom rectangular element were developed.

The convergence of the method was established and the natural frequencies were obtained for various boundary conditions and different modes. These results were

compared with those of other authors and theories and satisfactory agreement was found.

This method combines the advantage of finite element analysis and the precision of a formulation which uses displacement functions derived from thin plate theory.

A paper currently under preparation will deal with the dynamics of rectangular plates submerged in a fluid. A more general quadrilateral element will be used and further investigation will be done on the displacement function in order to predict the natural frequencies of anti-symmetrical modes.

2.9 REFERENCES

1. A. E. H. Love, *A Treatise on the Mathematical Theory of Elasticity*, Dover, New York (1944).
2. A. W. Leissa, *Vibration of Plates*, NASA, SP-160, 1969.
3. M. J. Turner, Clough, R. W. Martin and al., Stiffness and Deflection Analysis of Complex Structure. J. Aero Sci., 23, (Sept 1956), 805-823.
4. O. C. Zienkiewicz, *The Finite Element Method*, 3rd edn., Mc Graw Hill, New York, 1977
5. F. K. Bogner and al., A cylindrical shell element. AIAA J. 5, 745-750 (1967).
6. F. K. Bogner and al., The generation of interelement-compatible stiffness and mass matrices by the use of interpolation formulas. Proceeding of the Conference on Matrix Method in Structural Mechanics, Wright-Patterson Air Force Base/Air Force flight Dynamics Lab. TR-66-80 (1966).
7. J. L. Sanders, An improved first approximation theory for thin shell. NASA TR-24, 1959.
8. A. A. Lakis and M. P. Paidoussis, Dynamic analysis of axially non-uniform thin cylindrical shells, J. Mech. Eng. Sci. **14**, 49-71 (1972).
9. A. A. Lakis and M. P. Paidoussis, Free vibration of cylindrical shells partially filled with liquid, J. sound vib., **19,** 1-15 (1971).

10. A. A. Lakis and M. P. Paidoussis, Prediction or the response of a cylindrical shell to arbitrary of boundary-layer-induced random pressure field, J. sound vib., **25**, 1-27 (1972).

11. A. A. Lakis, Theoretical model of cylindrical structures containing turbulent flowing fluids, 2nd Int. Symp. on Finite Element Methods in Flow Problems, Santa margherita Ligure, Italy, June 1976.

12. A. A. Lakis, S. M. Sami and J. Rousellet, Turbulent two phases flow loop facility for predicting wall-pressure fluctuation and shell response, 24th Int. Instrument Symp. Albuquerque, New Mexico, May 1978.

13. A. A. Lakis and M. P. Paidoussis, Shell natural frequencies of the pickering steam generator, Anatomic Energy of Canada Ltd., AECL Report No. 4362, 1973.

14. A. A. Lakis and M. Sinno, Free vibration of axisymmetric and beam-like cylindrical shells partially filled with liquid, Int. j. numer. methods eng., **33**, 235-268 (1992).

15. A. Lakis and A. Laveau, Non-linear dynamic analysis of anisotropic cylindrical shells containing a flowing fluid, Int. J. solids struct. **28**, 1079-1094 (1991).

16. A. A. Lakis, P. Van Dyke and H. Ouriche, Dynamic analysis of anisotroppic fluid-filled conical shells, J. Fluids Struct. **6**, 135-162 (1992).

17. A. Lakis, N. Tuy, A. Laveau and A. Selmane, Analysis of axially non-uniform thin spherical shells, Int. Symp. STRUCOPT-COMPUMAT, Paris, France, 1989, pp. 80-85.

18. A. I. Martin, On the Vibration of Cantilever Plate. Quart. J. Mech. Appl. Math., vol. 9, pt 1, 1956, pp. 94-102.

19. B. Grinsted, Nodal Pattern Analysis. Proc. Inst. Mech. Eng., ser. A, vol. 166, 1952, pp.309-326.

20. R. Szelard, *Theory and Analysis of plates*, Prenctice-Hall, Englewood Cliffs, NJ, 1974.

2.10 NOTATION

List of symbol

a	length of the rectangular plate
A_i	defined by equation (2.8), i = 0, 1, 2, 3
b	width of the rectangular plate
B_j	defined by equation (2.8), j = 0, 1, 2, 3
C_i	defined by equation (2.6)
D	membrane stiffness, $Et/(1-\nu^2)$
E	Young's modulus
$E^{(k)}_{i,j}$	defined in equation (2.23), i = 1, 2, ..., 16 ; j = 1, 2, ..., 16
$f_{i,j}$	natural frequency (Hz)
$G^{(u)}_{i,j}$, $G^{(v)}_{i,j}$, $G^{(w)}_{i,j}$	defined by equation (2.23), i = 1, 2, ..., 16 ; j = 1, 2, ..., 16
K	bending stiffness, $Et^3/12(1-\nu^2)$
$L_{i,j}$	defined in equation (2.23), i = 1, 2, ..., 16 ; j = 1, 2, ..., 16
m	axial ode number parallel to the x-axis
$M_{i,j}$	defined in equation (2.23), i = 1, 2, ..., 16 ; j = 1, 2, ..., 16
$M_{x,x}$, M_n, $M_{y,y}$	bending moments of a rectangular plate
n	axial mode number parallel to the y-axis
N	number of finite elements
$N_{x,x}$, $N_{x,y}$, N_y	stress components of a rectangular plate
$P_{i,j}$	terms of the elasticity matrix, i =1, 2, ..., 6, j =1, 2, ..., 6
$S^{(u)}_{i,j}$, $S^{(v)}_{i,j}$, $S^{(w)}_{i,j}$	defined by equation (2.21), i = 1, 2, ..., 16 ; j = 1, 2, ..., 16

t	thickness of the rectangular plate
u_i, v_i, w_i	nodal displacements, $i = 1, \ldots, 4$
U, V, W	in-plane and normal displacement of a rectangular plate
x, y	length and width co-ordinate of the plate
$w_{i,x}$, $w_{i,y}$, $w_{i,xy}$	nodal rotations and twisting, $i = 1, \ldots, 4$
W_p	displacement function defined by equation (2.8)
δ_i	degree of freedom at node i, $i = 1, \ldots, 4$
ε_x, ε_y, ε_{xy}	deformations of the plate reference surface
κ_x, κ_y, κ_{xy}	changes in curvature and twisting of the plate reference surface
ρ	density of the plate material
υ	Poisson's ratio
ω	angular natural frequency, rad s^{-1}
Ω	non-dimensional frequency, $\omega a^2(\rho t/K)^{1/2}$
ψ	phase angle

List of matrices

[A]	defined by equation (2.12), given in Appendix II
[B]	defined by equation (2.14)
[C]	defined by equation (2.10)
[D]	defined by equation (2.14)
[G]	defined by equation (2.22)

$[k]$	stiffness matrix of one element
$[K]$	stiffness matrix of the total plate
$[m]$	mass matrix of one element
$[M]$	mass matrix of the total plate
$[N]$	defined by equation (2.13)
$[P]$	elasticity matrix
$[S]$	defined by equation (2.20)
$\{\varepsilon\}$	strain vector
$\{\sigma\}$	stress vector
$\{\delta_i\}$	degrees of freedom at node i
$\{\delta_T\}$	degrees of freedom for the total plate
$\{\delta_{0,1}\}$	Amplitude of the plate motion

APPENDIX I

The matrix [A] is defined by:

$$
\begin{bmatrix}
0 & 0 & 0 & 1 & 0 & 0 & 0 & 0 & 0 & 0 & 0 & 0 & 0 & 0 & 0 & 0 & 0 & 0 & 0 & 0 & 0 & 0 & 0 & 0 \\
0 & 0 & 0 & 0 & 0 & 0 & 0 & 1 & 0 & 0 & 0 & 0 & 0 & 0 & 0 & 0 & 0 & 0 & 0 & 0 & 0 & 0 & 0 & 0 \\
0 & 0 & 0 & 0 & 0 & 0 & 0 & 0 & 0 & 0 & 0 & 0 & 0 & 0 & 0 & 0 & 0 & 0 & 0 & 0 & 0 & 0 & 0 & 1 \\
0 & 0 & 0 & 0 & 0 & 0 & 0 & 0 & 0 & 0 & 0 & 0 & 0 & 0 & 0 & 0 & 0 & 0 & 0 & \frac{1}{a} & 0 & 0 & 0 & 0 \\
0 & 0 & 0 & 0 & 0 & 0 & 0 & 0 & 0 & 0 & 0 & 0 & 0 & 0 & 0 & 0 & 0 & 0 & 0 & 0 & 0 & 0 & \frac{1}{b} & 0 \\
0 & 0 & 0 & 0 & 0 & 0 & 0 & 0 & 0 & 0 & 0 & 0 & 0 & 0 & 0 & 0 & 0 & 0 & \frac{1}{a \cdot b} & 0 & 0 & 0 & 0 & 0 \\
0 & 1 & 0 & 1 & 0 & 0 & 0 & 0 & 0 & 0 & 0 & 0 & 0 & 0 & 0 & 0 & 0 & 0 & 0 & 0 & 0 & 0 & 0 & 0 \\
0 & 0 & 0 & 0 & 0 & 1 & 0 & 1 & 0 & 0 & 0 & 0 & 0 & 0 & 0 & 0 & 0 & 0 & 0 & 0 & 0 & 0 & 0 & 0 \\
0 & 0 & 0 & 0 & 0 & 0 & 0 & 0 & 0 & 0 & 0 & 1 & 0 & 0 & 0 & 1 & 0 & 0 & 0 & 1 & 0 & 0 & 0 & 1 \\
0 & 0 & 0 & 0 & 0 & 0 & 0 & 0 & 0 & 0 & 0 & \frac{3}{a} & 0 & 0 & 0 & \frac{2}{a} & 0 & 0 & 0 & \frac{1}{a} & 0 & 0 & 0 & 0 \\
0 & 0 & 0 & 0 & 0 & 0 & 0 & 0 & 0 & 0 & \frac{1}{b} & 0 & 0 & 0 & \frac{1}{b} & 0 & 0 & 0 & \frac{1}{b} & 0 & 0 & 0 & \frac{1}{b} & 0 \\
0 & 0 & 0 & 0 & 0 & 0 & 0 & 0 & 0 & 0 & \frac{3}{a \cdot b} & 0 & 0 & 0 & \frac{2}{a \cdot b} & 0 & 0 & 0 & \frac{1}{a \cdot b} & 0 & 0 & 0 & 0 & 0 \\
1 & 1 & 1 & 1 & 0 & 0 & 0 & 0 & 0 & 0 & 0 & 0 & 0 & 0 & 0 & 0 & 0 & 0 & 0 & 0 & 0 & 0 & 0 & 0 \\
0 & 0 & 0 & 0 & 1 & 1 & 1 & 1 & 0 & 0 & 0 & 0 & 0 & 0 & 0 & 0 & 0 & 0 & 0 & 0 & 0 & 0 & 0 & 0 \\
0 & 0 & 0 & 0 & 0 & 0 & 0 & 0 & 1 & 1 & 1 & 1 & 1 & 1 & 1 & 1 & 1 & 1 & 1 & 1 & 1 & 1 & 1 & 1 \\
0 & 0 & 0 & 0 & 0 & 0 & 0 & 0 & \frac{3}{a} & \frac{3}{a} & \frac{3}{a} & \frac{3}{a} & \frac{2}{a} & \frac{2}{a} & \frac{2}{a} & \frac{2}{a} & \frac{1}{a} & \frac{1}{a} & \frac{1}{a} & \frac{1}{a} & 0 & 0 & 0 & 0 \\
0 & 0 & 0 & 0 & 0 & 0 & 0 & 0 & \frac{3}{b} & \frac{2}{b} & \frac{1}{b} & 0 & \frac{3}{b} & \frac{2}{b} & \frac{1}{b} & 0 & \frac{3}{b} & \frac{2}{b} & \frac{3}{b} & 0 & \frac{3}{b} & \frac{2}{b} & \frac{1}{b} & 0 \\
0 & 0 & 0 & 0 & 0 & 0 & 0 & 0 & \frac{9}{a \cdot b} & \frac{6}{a \cdot b} & \frac{3}{a \cdot b} & 0 & \frac{6}{a \cdot b} & \frac{4}{a \cdot b} & \frac{2}{a \cdot b} & 0 & \frac{3}{a \cdot b} & \frac{2}{a \cdot b} & \frac{1}{a \cdot b} & 0 & 0 & 0 & 0 & 0 \\
0 & 0 & 1 & 1 & 0 & 0 & 0 & 0 & 0 & 0 & 0 & 0 & 0 & 0 & 0 & 0 & 0 & 0 & 0 & 0 & 0 & 0 & 0 & 0 \\
0 & 0 & 0 & 0 & 0 & 0 & 1 & 1 & 0 & 0 & 0 & 0 & 0 & 0 & 0 & 0 & 0 & 0 & 0 & 0 & 0 & 0 & 0 & 0 \\
0 & 0 & 0 & 0 & 0 & 0 & 0 & 0 & 0 & 0 & 0 & 0 & 0 & 0 & 0 & 0 & 0 & 0 & 0 & 0 & 1 & 1 & 1 & 1 \\
0 & 0 & 0 & 0 & 0 & 0 & 0 & 0 & 0 & 0 & 0 & 0 & 0 & 0 & 0 & 0 & \frac{1}{a} & \frac{1}{a} & \frac{1}{a} & \frac{1}{a} & 0 & 0 & 0 & 0 \\
0 & 0 & 0 & 0 & 0 & 0 & 0 & 0 & 0 & 0 & 0 & 0 & 0 & 0 & 0 & 0 & 0 & 0 & 0 & 0 & \frac{3}{b} & \frac{2}{b} & \frac{1}{b} & 0 \\
0 & 0 & 0 & 0 & 0 & 0 & 0 & 0 & 0 & 0 & 0 & 0 & 0 & 0 & 0 & 0 & \frac{3}{a \cdot b} & \frac{2}{a \cdot b} & \frac{1}{a \cdot b} & 0 & 0 & 0 & 0 & 0
\end{bmatrix}
$$

CHAPITRE III

ARTICLE 2[2]

VIBRATION ANALYSIS OF RECTANGULAR PLATES SUBMERGED IN FLUIDS

E. Charbonneau and **A. A. Lakis**

Department of Mechanical Engineering, École Polytechnique de Montréal, Campus de l'Université de Montréal, C.P. 6079, Succ. Centre-Ville, Montréal, Québec, Canada H3C 3A7

3.1 SUMMARY

A theory is presented to study the dynamic characteristics of flat horizontal rectangular plates vibrating in fluids. The effect of the boundary conditions and the depth of submergence of the plates have been studied. The formulation used is a combination of the finite element method and classical plate theory. The displacement functions are derived from exact solutions of Sanders' shell equations and expanded in power series. The velocity potential and Bernoulli's equation for a fluid finite element yield an expression for fluid pressure as a function of the nodal displacements of the plate element and inertial force of the fluid at rest. An analytical integration of the fluid

[2] Soumis pour publication à *Journal of Fluids and Structures*

pressure over the fluid element leads to the mass matrix. Calculations are given to validate the application of the method. Reasonable agreement is found with other theories and experiments.

3.2 INTRODUCTION

Knowledge of the vibration characteristics of rectangular plates submerged or in contact with fluids is of considerable interest since they are used in many applications, such as the naval, aerospace and construction industries. The dynamics of a structure interacting with fluid were first described by Lamb (1945). Later, Lindholm et al. (1965) carried out an extensive experimental study of the response of cantilevered plates in air and in water. The results were compared with theoretical predictions based on simple beam theory or thin plate theory and the chordwise hydrodynamic strip theory. Leissa (1973) gives some references for shell-like containers partially filled with liquids.

However, there seems to be a relatively limited number of studies of free surface effects on structures. More recently, Fu and Price (1987) studied the vibration response of cantilevered plates partially or totally immersed within the fluid. They used a combination of the finite element method and a singularity distribution panel approach to examine the effects of the free surface, frequency and length or depth of plate immersion on the dynamic characteristics of the plate. Robinson and Palmer (1990) give a method for modal analysis of a rectangular plate floating on a fluid. They

deduced the velocity or pressure distribution function of the fluid by solving the wave equation with the unsteady Bernoulli equation applied at the fluid-plate interface. Following the same approach, Soedel and Soedel (1994) give an analytical solution for a simply supported plate supporting a liquid with a freely sloshing surface. Amabili (1996) used the Rayleigh-Ritz approach to obtain an analytical solution for the case of a fluid domain of finite depth which either has a free surface or is constrained by rigid walls. The effect of the depth of the fluid domain on the added mass factor, natural frequencies and mode shapes is studied. Haddara and Cao (1996) used the same philosophy to investigate analytically and experimentally the dynamic response of submerged rectangular plates with various boundary conditions. They provide an analytical added mass factor depending on the height of the free surface and the depth of the fluid under the plate. Moreover, they show that the boundary conditions have little effect on the change in natural frequency of the plate under study.

Lakis and Paidoussis (1971) studied the free vibration of a cylindrical shell partially filled with liquid using a combination of finite element analysis and classical shell theory. The objective was to determine the specific displacement functions which best represent the real deformations. To continue on the subject, Lakis and Neagu (1997) studied the free surface effects on the dynamics of a cylindrical shell partially filled with liquid. The kinetic and potential energies of the fluid are evaluated in order to establish the influence of the surface oscillation on fluid-shell vibration.

Following the same idea, we will present in this paper a method to study the dynamics of thin rectangular plates in contact with fluids at rest. In a previous paper, (Charbonneau and Lakis 1999) a combination of finite element method and classical plate theory has been used to derive a rectangular plate finite element that is compatible with both the plate equations of motion and the fluid wave equations. In this article, we are solving the Laplace equation for the velocity potential with a free surface by applying the Bernoulli equation at the fluid-plate interface, which yields an expression for fluid pressure as a function of the nodal displacements of the plate element. An analytical integration of the fluid pressure over the liquid element leads to the fluid mass matrix. This fluid mass matrix is later used with the plate mass and stiffness matrices to compute natural frequencies and mode shapes of rectangular plates with different boundary conditions.

3.3 DISPLACEMENT FUNCTIONS

To find out the equilibrium equations of the plate, we will use Sander's equations (1959) for cylindrical shells and assume the radius to be infinite, $\theta = y$ and $rd\theta = dy$. These three new equations will take into account membrane effects as well as bending effects. The equations of motion in terms of the in-plane and normal displacements (U, V, W) of the plate's mean surface (Figure 3.1) and in terms of element P_{ij} of the isotropic matrix of elasticity [P] are

$$P_{22}\frac{\partial^2 V}{\partial y^2}+P_{21}\frac{\partial^2 U}{\partial x\partial y}+P_{33}\left(\frac{\partial^2 U}{\partial x\partial y}+\frac{\partial^2 V}{\partial x^2}\right)=0$$

$$P_{11}\frac{\partial^2 U}{\partial x^2}+P_{12}\frac{\partial^2 V}{\partial x\partial y}+P_{33}\left(\frac{\partial^2 V}{\partial x\partial y}+\frac{\partial^2 U}{\partial y^2}\right)=0 \qquad (3.1)$$

$$P_{44}\frac{\partial^4 W}{\partial x^4}+\frac{\partial^4 W}{\partial x^2\partial y^2}\left(P_{45}+P_{54}+2P_{66}\right)+P_{55}\frac{\partial^4 W}{\partial y^4}=0$$

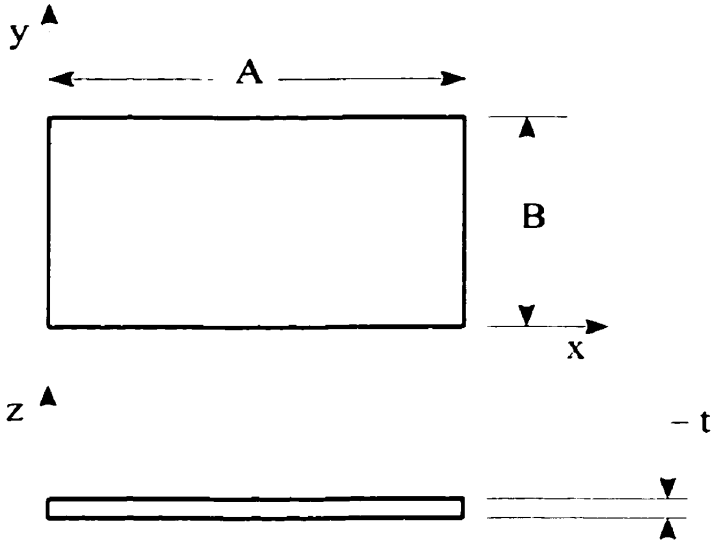

Fig. 3.1. Geometry of rectangular plate

The strain-displacement relation is given by

$$\begin{pmatrix} \varepsilon_x \\ \varepsilon_y \\ 2\varepsilon_{xy} \\ \kappa_x \\ \kappa_y \\ \kappa_{xy} \end{pmatrix} = \begin{Bmatrix} \dfrac{\partial U}{\partial x} \\ \dfrac{\partial V}{\partial y} \\ \dfrac{\partial V}{\partial x} + \dfrac{\partial U}{\partial y} \\ -\dfrac{\partial^2 W}{\partial x^2} \\ -\dfrac{\partial^2 W}{\partial y^2} \\ -\dfrac{\partial^2 W}{\partial x \partial y} \end{Bmatrix} \tag{3.2}$$

The rectangular plate finite element used is shown in Figure 3.2. This four-node element is defined by twenty-four degrees of freedom, six degrees by node. Those degrees of freedom, shown in Figure 3.2, are: three displacements (U, V, W), two rotations ($\partial W/\partial x$, $\partial W/\partial y$) and twisting ($\partial^2 W/\partial x \partial y$).

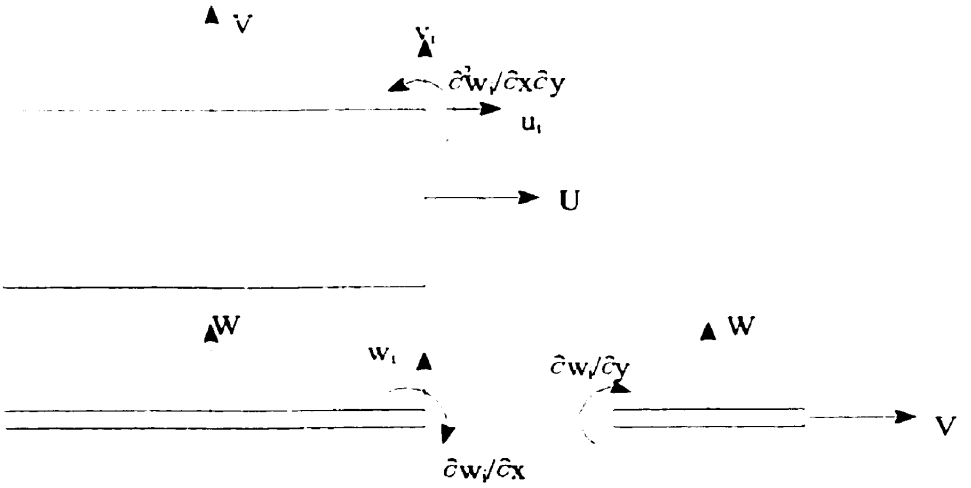

Fig. 3.2. Displacements and degrees of freedom of a rectangular plate

The assumed displacement functions that will represent the motion of the plate are (Charbonneau and Lakis 1999)

$$U(x,y) = C_1 + C_2\frac{x}{a} + C_3\frac{y}{b} + C_4\frac{xy}{ab} \tag{3.3a}$$

$$V(x,y) = C_5 + C_6\frac{x}{a} + C_7\frac{y}{b} + C_8\frac{xy}{ab} \tag{3.3b}$$

$$W(x,y) = \left[\sum_{i=0}^{3}\frac{A_i}{i!}\left(\frac{x}{a}\right)^i\right]\left[\sum_{j=0}^{3}\frac{B_j}{j!}\left(\frac{y}{b}\right)^j\right] \tag{3.3c}$$

$$W(x,y,t) = \sum_{j=1}^{n} C_j e^{\pi\left(\frac{x}{A}+\frac{y}{B}+\omega t\right)} \tag{3.3d}$$

where U(x, y) and V(x, y) describe the membrane behaviour (eq. 3.3a and 3.3b) and W(x, y) the normal displacement of the plate. The functions U and V contain the same number of unknown parameters C_i as the number of degrees of freedom of a membrane element (2 x 4 = 8). The polynomials representing the membrane displacements are low order polynomials, but converge monotonically to the exact solution. Since it is a complex matter to find the characteristic equation of the solution of the bi-harmonic governing the bending of a plate (eq. 3.3d), we expanded the solution in a Taylor series (eq. 3.3c). The A_i and B_j are the 16 unknown constants representing the 16 degrees of freedom in bending for a plate. Furthermore, when using a power series to express the displacement function, we approach more closely the "exact" solution of the bending equation than Bogner et al. (1966) did. The two displacements functions are compared to exact equation in figure 3.3.

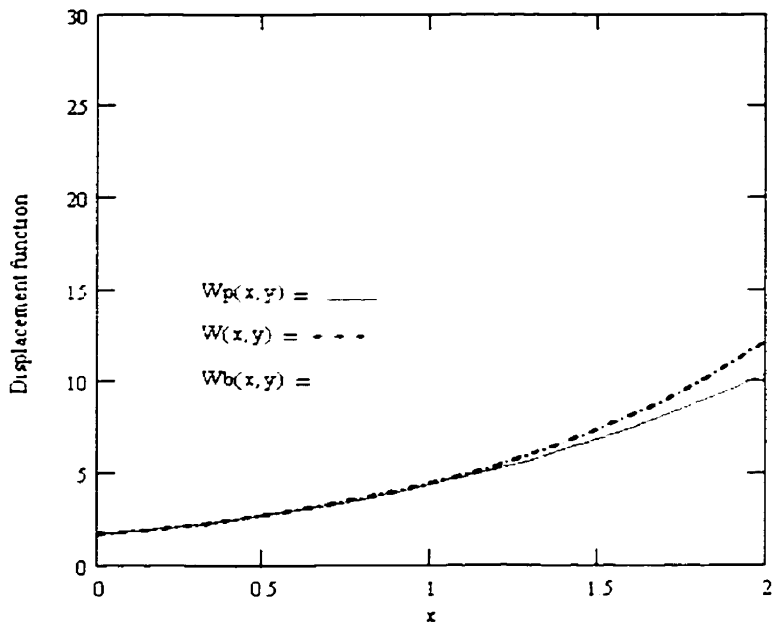

Fig. 3.3. Comparison of displacement functions: equation (3.3) $W_p(x,y)$: ——; Bogner 1966 $W_b(x,y)$: — —; and the exact solution equation $W(x,y)$: – –.

Now, we can write the displacement functions in the matrix form

$$\begin{Bmatrix} U \\ V \\ W \end{Bmatrix} = [R] \quad \{C\} \tag{3.4}$$

where [R] is a 3x24 matrix whom components are the x and y terms of equations (3.3) without the unknown constants. The vector {C} is given by:

$$\{C\} = \{C_1, \ldots, C_{24}\}^t \tag{3.5}$$

To determine these constants, we need to define twenty-four boundary conditions for the finite element. These twenty-four boundary conditions will be the twenty-four degrees of freedom element, which means six degrees of freedom per node as follows:

$$\{\delta_1, \delta_2, \delta_3, \delta_4\}^t = \{u_1, v_1, w_1, w_{1,x}, w_{1,y}, w_{1,xy}, u_2, v_2, w_2, w_{2,x}, w_{2,y}, w_{2,xy},$$

$$u_3, v_3, w_3, w_{3,x}, w_{3,y}, w_{3,xy}, u_4, v_4, w_4, w_{4,x}, w_{4,y}, w_{4,xy}\} \quad (3.6)$$

where the δ_is are the generalized nodal displacement and $w_{i,x}$ is the derivative of w_i respect to x and so on. Then, a transformation matrix [A] has to be defined to relate the displacement functions $\{C_i\}$ and the nodal displacements $\{\delta_i\}$:

$$\{\delta_i\} = [A]\{C_i\} \quad (3.7)$$

[A] is a 24x24 matrix listed in Appendix A. The terms of matrix [A] are obtained from matrix [R] by going from node 1 to node 4 and setting the value of x to 0 or a, and, y to 0 or b. Now, multiplying equation (3.7) by $[A]^{-1}$ and substituting into equation (3.4) we obtain

$$\begin{Bmatrix} U \\ V \\ W \end{Bmatrix} = [R] \quad [A]^{-1} \begin{Bmatrix} \delta_1 \\ \delta_2 \\ \delta_3 \\ \delta_4 \end{Bmatrix} = [N] \begin{Bmatrix} \delta_1 \\ \delta_2 \\ \delta_3 \\ \delta_4 \end{Bmatrix} \quad (3.8)$$

where [N] is the displacement functions matrix for a finite element of rectangular plate.

3.4 MASS AND STIFFNESS MATRICES FOR AN EMPTY FINITE ELEMENT

The strains are related to the displacements through equation (3.2); accordingly, we may now express $\{\varepsilon\}$ in terms of the generalized nodal displacements δ_i

$$\{\varepsilon\} = [D] \quad [R] \quad [A^{-1}] \quad \begin{Bmatrix} \delta_1 \\ \delta_2 \\ \delta_3 \\ \delta_4 \end{Bmatrix} = [B] \quad \begin{Bmatrix} \delta_1 \\ \delta_2 \\ \delta_3 \\ \delta_4 \end{Bmatrix} \tag{3.9}$$

where [D] is a matrix containing the derivative operators from equation (3.2).

The corresponding stresses may be related to the strains by the elasticity matrix [P]:

$$\{\sigma\} = [P] \quad \{\varepsilon\} = [P] \quad [B] \quad \begin{Bmatrix} \delta_1 \\ \delta_2 \\ \delta_3 \\ \delta_4 \end{Bmatrix} \tag{3.10}$$

where [P] is a 6x6 symmetric elasticity matrix. In the case of an isotropic material there will be no coupling between membrane and bending effects and the only non-vanishing terms are:

$$\begin{aligned} P_{11} = P_{22} = D \quad & P_{44} = P_{55} = K \\ P_{12} = P_{21} = \nu D \quad & P_{45} = P_{54} = <K \\ P_{33} = \frac{(1-\nu)}{2} D \quad & P_{66} = \frac{(1-\nu)}{2} K \end{aligned} \tag{3.11}$$

where D and K are respectively the membrane and bending stiffness defined as

$$D = \frac{Et}{1-\nu^2} \qquad K = \frac{Et^3}{12(1-\nu^2)}$$

E being the young's modulus, υ Poisson's ratio and t the plate thickness.

The mass and stiffness matrices $[m_s]$ and $[k_s]$ respectively, for one finte element may be written as follows:

$$[m_s] = \rho_s \quad t \int_0^a \int_0^b [N]^T \quad [N] \quad dA \tag{3.12}$$

$$[k_s] = \int_0^a \int_0^b [B]^T [P] \quad [B] \quad dA \tag{3.13}$$

where ρ_s is the density of the plate material, t is the thickness, dA a surface element, [P] the elasticity matrix and the matrices [N] and [B] are obtained from equations (3.8) and (3.9) respectively.

The matrices $[m_s]$ and $[k_s]$ were obtained analytically by carrying out the necessary matrix operations and integration over x and y in equations (3.12) and (3.13). The global matrices $[M_s]$ and $[K_s]$ may be assembled, respectively, by superimposing the mass $[m_s]$ and stiffness $[k_s]$ matrices for each individual plate finite element. See Charbonneau and Lakis (1999) for more details.

3.5 BEHAVIOUR OF THE FLUID-PLATE INTERACTION

3.5.1 Equations of motion

The dynamic behavior of a rectangular plate subjected to a fluid pressure field (figure 3.4) can be represented by the following system:

$$[[M_s]-[M_f]]\ \{\ddot{\Delta}\}-[C_f]\ \{\dot{\Delta}\}+[[K_s]-[K_f]]\ \{\Delta\}=\{F(t)\} \tag{3.14}$$

where $\{\Delta\}$ is the displacement vector, $[M_s]$ and $[K_s]$ are respectively the mass and stiffness matrices of the system in vacuum; $[M_f]$, $[C_f]$ and $[K_f]$ are the mass, damping and stiffness matrices that takes into account the inertial Coriolis and centrifugal forces of the liquid flow and $\{F\}$ represents the external forces.

In the case of a liquid at rest the matrices $[C_f]$, $[K_f]$ and $\{F(t)\}$ are null and equation (3.14) takes the form

$$[[M_s]-[M_f]]\ \{\ddot{\Delta}\}+[K_s]\ \{\Delta\}=0 \tag{3.15}$$

Therefore, when a structure is submerged in a fluid at rest, the interaction between the fluid and the structure is purely inertial.

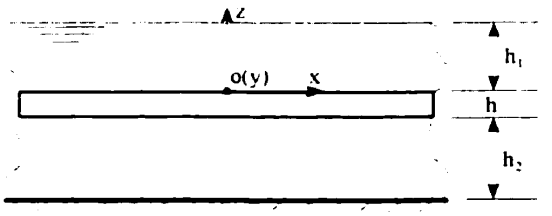

Fig. 3.4. Rectangular plate submerged in a body of fluid.

3.5.2 Assumptions

We will assume that the structure is submerged in a fluid at rest. Moreover, the mathematical model, which is developed here, is based on the following hypotheses: (i) the fluid flow is potential. (ii) vibration is linear, (iii) the fluid is incompressible.

3.5.3 Dynamic pressure at the plate-fluid interface

With the assumptions of section 4.2, the velocity potential must satisfy the Laplace equation which is, in the rectangular coordinate system, as follows

$$\nabla^2 \Phi = \frac{\partial^2 \Phi}{\partial x^2} + \frac{\partial^2 \Phi}{\partial y^2} + \frac{\partial^2 \Phi}{\partial z^2} = 0 \tag{3.16}$$

Φ is the potential function that represents the velocity potential.

At the fluid-plate interfaces, the impermeability condition ensures contact between the plate and the fluid. This should be

$$\left.\frac{\partial \Phi}{\partial z}\right|_{z=0} = \left.\frac{\partial \Phi}{\partial z}\right|_{z=-h} = \frac{\partial W}{\partial t} \tag{3.17}$$

From the theory of plates, Charbonneau and Lakis (1999), we have

$$W(x, y, t) = \sum_{j=1}^{n} C_j e^{\pi i\left(\frac{x}{A} + \frac{y}{B} - \omega t\right)} \tag{3.18}$$

where i is the complex number, $i^2 = -1$.

Assuming then,

$$\Phi(x, y, z, t) = \sum_{j=1}^{n} F_j(z) S_j(x, y, t) \tag{3.19}$$

and applying the impermeability condition, equation (3.17), to equation (3.18) and (3.19), we determine the function $S_j(x,y,t)$. The dynamic pressure at the fluid-plate interface is given by the Bernoulli's equation as follows:

$$P = \rho_f \frac{\partial \Phi}{\partial t} \tag{3.20}$$

Reintroducing $S_j(x,y,t)$ term into equation (3.19) and substituting it into Bernoulli's equation (3.20), we find a relation for the dynamic pressure as a function of the displacement W_j and the function $F_j(z)$:

$$P|_{z=0} = \rho_f \sum_{j=1}^{n} \frac{F_{1,j}(0)}{F'_{1,j}(0)} \ddot{W}_j \quad \text{, at the plate top surface (see figure 3.4)} \tag{3.21a}$$

$$P|_{z=-h} = -\rho_f \sum_{j=1}^{n} \frac{F_{2,j}(-h)}{F'_{2,j}(-h)} \ddot{W}_j \quad \text{, at the plate bottom surface} \tag{3.21b}$$

where $F_{i,j}(z)$ is to be determined and $(\,)'$ and $(\,)^{\bullet}$ represent $\partial(\,)/\partial z$ and $\partial(\,)/\partial t$ respectively.

By using again relations (3.18) and (3.19), one can express the velocity potential in term of the plate motion and introduce this in the Laplace equation, (3.16), to get

$$\frac{d^2 F_j(z)}{dz^2} - \mu_r^2 F_j(z) = 0 \tag{3.22}$$

where $\mu_r = \pi \sqrt{\frac{1}{A^2} + \frac{1}{B^2}}$ and, A and B are the plate length and width respectively.

To solve equation (3.22), we will need three boundary conditions for the fluid. The first one is given by equation (3.17). The second one is defined by equation (3.24) and gives the free surface behavior

$$\left.\frac{\partial \Phi}{\partial z}\right|_{z=h_1} = \frac{1}{g} \frac{\partial^2 \Phi}{\partial t^2} \tag{3.24}$$

where g is the gravitational accelaration. At the bottom end of the fluid (see figure 3.4), the normal componenent of velocity is zero, i.e.

$$\left.\frac{\partial \Phi}{\partial z}\right|_{z=-(h+h_2)} = 0 \tag{3.25}$$

The solution of equation (3.22) consits of two parts: one for the fluid over the plate,$F_{1,J}(z)$, and a second one for the fluid under the plate, $F_{2,J}(z)$. The general solution of equation (3.22) is given by:

$$F_1(z) = A_1 e^{\mu z} + A_2 e^{-\mu z} \tag{3.26}$$

where A_1 and A_2 are constants.

Applying the boundary conditions equations (3.17), (3.24) and (3.25) gives a unique solution

$$F_1(z) = -\frac{\left(C_1 e^{\mu(z-h_1)} + e^{-\mu(z-h_1)}\right)}{\mu\left(e^{\mu h_1} - C_1 e^{-\mu h_1}\right)} F_1'(0) \tag{3.27}$$

where $C_1 = \dfrac{g\mu + \omega_f^2}{g\mu - \omega_f^2}$ and ω_f is the natural frequency of the plate in fluid.

Similarly, a unique solution can be found for the fluid under the plate

$$F_2(z) = \frac{\left(e^{\mu(2h-2h_2+z)} + e^{-\mu z}\right)}{\mu\left(e^{\mu(h-2h_2)} - e^{\mu h}\right)} F_2'(-h) \tag{3.28}$$

Now, before expressing the total pressure at the plate interface, we still have to determine the value of C_1 as a function of ω_f. Figure 3.5 shows the behavior of C_1 as a function of ω_f. As can be seen, C_1 tends to a value of -1 when ω_f tends to infinity (Haddara and Cao 1996). Figure 3.5 indicates that, we can use the a value of $C_1 = -1$ when ω_f is greater than 10 Hz. Figure 3.5 also brings us to the conclusion that, when we

have a system with natural frequencies higher than 10 Hz, the natural frequencies do not really depend on their mode shape but on the plate geometry, the fluid properties and the fluid heights under and above the plate. When we have a system with natural frequencies lower than 10 Hz, the value of C_1 should be corrected as close as possible to its exact value through an iterative procedure.

Finally, the total pressure at the plate interface is taken as the sum of equation (3.21a) and (3.21b)

$$P_T = \rho_f \left[\frac{\left(C_1 e^{-\mu h_1} + e^{\mu h_1}\right)}{\mu\left(e^{\mu h_1} - C_1 e^{-\mu h_1}\right)} - \frac{\left(e^{\mu(h+2h_2)} + e^{\mu h}\right)}{\mu\left(e^{\mu(h+2h_2)} - e^{\mu h}\right)} \right] \sum_{i=1}^{n} \ddot{W}_i \tag{3.29}$$

where the ratios $\frac{F_1(0)}{F_1'(0)}$ and $\frac{F_2(-h)}{F_2'(-h)}$ are defined by evaluating equations (3.27) and (3.28) at z = 0 and z = -h respectively. For the sake of simplicity, in equation (3.29), we considered the fluid over and under the plate to be the same, but in reality the two fluids could be quite different.

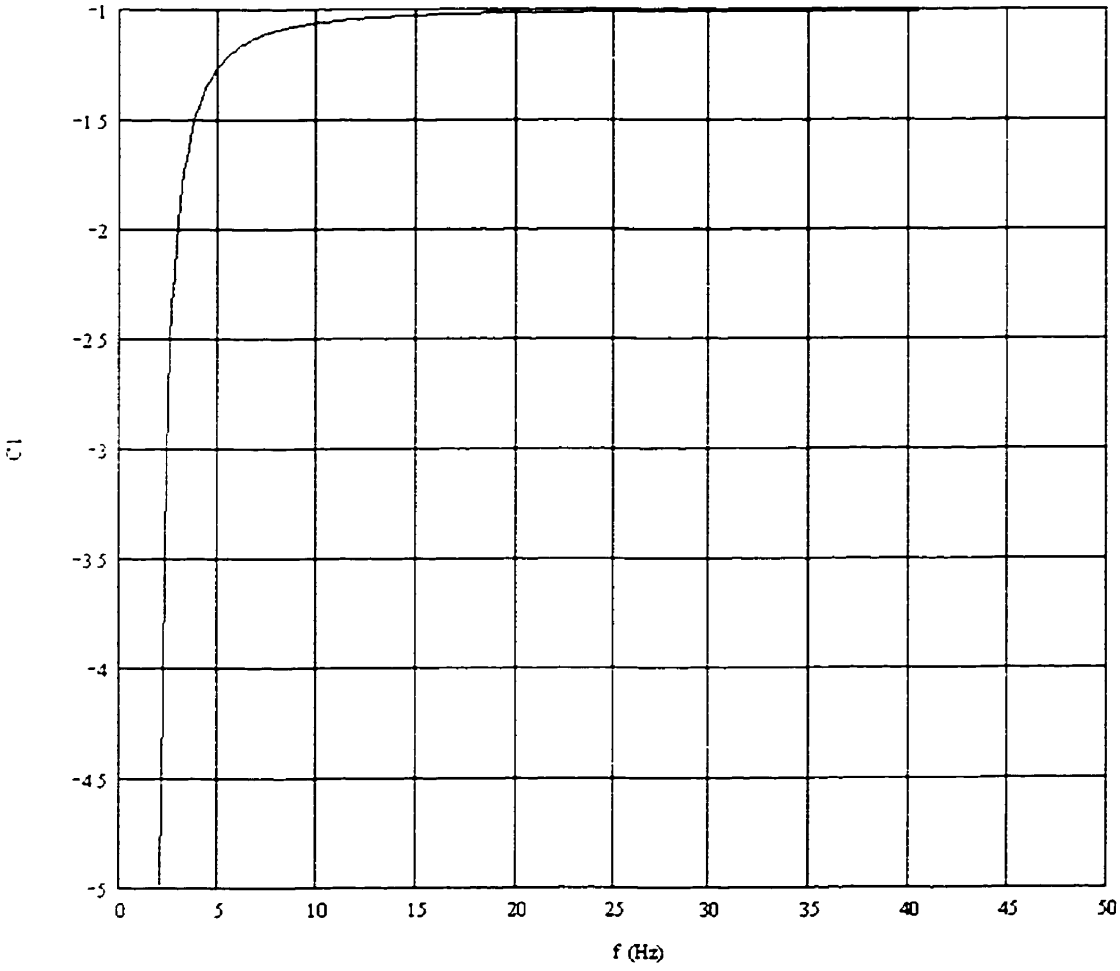

Fig. 3.5. $C_1 = \dfrac{g\mu + (2\pi f)^2}{g\mu - (2\pi f)^2}$ in function of the natural frequency of a plate in fluid.

We can rewrite equation (3.29) as

$$P_T = \rho_f Z \sum_{i=1}^{n} \ddot{W}_i \tag{3.30}$$

where $Z = \left[\dfrac{\left(C_1 e^{-\mu h_1} + e^{\mu h_1}\right)}{\mu\left(e^{\mu h_1} - C_1 e^{-\mu h_1}\right)} - \dfrac{\left(e^{\mu(h+2h_2)} + e^{\mu h}\right)}{\mu\left(e^{\mu(h+2h_2)} - e^{\mu h}\right)} \right]$.

3.6 FLUID MASS MATRIX ABOVE AND UNDER THE PLATE

By intoducing the displacement function (3.8) into the dynamic pressure expression (3.30) and performing the matrix operation required by the finite element method, the mass matrix for the fluid element is obtained by evaluating the following integral:

$$\int_A [N]^T \{P_T\} dA \tag{3.31}$$

leading to

$$[m_f] = \rho_f Z [A^{-1}]^T [S_f] [A^{-1}] \tag{3.32}$$

The matrix [A] is defined by equation (3.7) and $[S_f]$ is a 24 x 24 real symmetric matrix partitioned as follow

$$[S_f] = \begin{bmatrix} S^{(u)}_{4\times4} & \vdots & 0 & \vdots & 0 \\ \cdots & \vdots & \cdots & \vdots & \cdots \\ 0 & \vdots & S^{(v)}_{4\times4} & \vdots & 0 \\ \cdots & \vdots & \cdots & \vdots & \cdots \\ 0 & \vdots & 0 & \vdots & S^{(w)}_{16\times16} \end{bmatrix} \tag{3.33}$$

The elements of the symmetric submatrices are given by

$$S_{ij}^{(u)} = S_{ij}^{(v)} = 0$$

$$S_{ij}^{(w)} = B_{ij}\, a\, b \tag{3.34}$$

where the constants B_{ij} 's are found in table 3.1 and a and b are respectively the length and width of an element.

Table 3.1. Constant for symmetric submatrices.

i	j	B_{ij}	i	j	B_{ij}	i	j	B_{ij}	i	j	B_{ij}	i	j	B_{ij}
1	1	1.63504	3	3	1.756	5	9	1.2016	8	10	1.48	12	15	[illegible]
1	2	1.18144	3	4	1.504	5	10	1.576	8	11	1.16	12	16	[illegible]
1	3	1.7560	3	5	1.2160	5	11	1.240	8	12	1.8	13	13	1.252
1	4	1.6048	3	6	1.576	5	12	1.192	8	13	1.144	13	14	1.72
1	5	1.18144	3	7	1.216	5	13	1.1512	8	14	1.36	13	15	1.36
1	6	1.5184	3	8	1.144	5	14	1.432	8	15	1.12	13	16	1.24
1	7	1.2160	3	9	1.960	5	15	1.180	8	16	1.6	14	14	1.20
1	8	1.1728	3	10	1.240	5	16	1.144	9	9	1.756	14	15	1.8
1	9	1.7560	3	11	1.90	6	6	1.448	9	10	1.216	14	16	1.6
1	10	1.2160	3	12	1.60	6	7	1.160	9	11	1.90	15	15	1.3
1	11	1.960	3	13	1.720	6	8	1.120	9	12	1.72	15	16	[illegible]
1	12	1.720	3	14	1.192	6	9	1.576	9	13	1.504	16	16	1
1	13	1.6048	3	15	1.72	6	10	1.160	9	14	1.144			
1	14	1.1728	3	16	1.48	6	11	1.64	9	15	1.60			
1	15	1.720	4	4	1.252	6	12	1.48	9	16	1.48			
1	16	1.576	4	5	1.1728	6	13	1.432	10	10	1.60			
2	2	1.5040	4	6	1.432	6	14	1.120	10	11	1.24			
2	3	1.2016	4	7	1.144	6	15	1.48	10	12	1.18			
2	4	1.1512	4	8	1.72	6	16	1.36	10	13	1.144			
2	5	1.5184	4	9	1.720	7	7	1.60	10	14	1.40			
2	6	1.1440	4	10	1.180	7	8	1.40	10	15	1.16			
2	7	1.576	4	11	1.60	7	9	1.240	10	16	1.12			
2	8	1.432	4	12	1.36	7	10	1.64	11	11	1.9			
2	9	1.2160	4	13	1.576	7	11	1.24	11	12	1.6			
2	10	1.600	4	14	1.144	7	12	1.16	11	13	1.60			
2	11	1.240	4	15	1.48	7	13	1.180	11	14	1.16			
2	12	1.180	4	16	1.24	7	14	1.48	11	15	1.6			
2	13	1.1728	5	5	1.5040	7	15	1.18	11	16	[illegible]			
2	14	1.480	5	6	1.1440	7	16	1.12	12	12	1.3			
2	15	1.192	5	7	1.600	8	8	1.20	12	13	1.48			
2	16	1.144	5	8	1.480	8	9	1.192	12	14	1.12			

3.7 EIGENVALUE AND EIGENVECTOR PROBLEM

Once the stiffness and the mass matrices for the structure and the fluid have been obtained it is possible to construct the global matrices for the complete plate using finite element assembly technique. If N is the number of nodes then $[M_s]$, $[M_f]$ and $[K_s]$ are three matrices of order 6N. In the case of free vibration, the equations of motion are:

$$[[M_s]-[M_f]]\left\{\ddot{\delta}_T\right\}+[K_s]\left\{\delta_T\right\}=\{0\} \tag{3.35}$$

where $\{\delta\}_T$ is the vector for global displacements of the whole shell.

$$\{\delta_T\} = \{\delta_1, \delta_2, \ldots, {}_N\delta\}^t \tag{3.36}$$

N being the number of nodes. By specifying

$$\{\delta_T\} = \{\delta_{0,T}\} \sin(\omega_f t + \psi) \tag{3.37}$$

where ω_f is natural angular frequency and ψ is the phase angle.

By introducing equation (3.35) and (3.36), we obtain the typical eigenvalue problem:

$$\text{Det}\ [\ [K_s] - \omega_f^2\ [M_s - M_f]\ ] = 0 \tag{3.38}$$

The resolution of system (3.38) yields to simultaneously the bending and in plane modes. The shape of the eigenvector for each mode will allow us to differentiate the bending modes from the in plane modes. The natural frequencies of the bending modes will be lowered by the contributing fluid inertia $[M_f]$.

3.8 CALCULATIONS AND DISCUSSIONS

Calculations have already been done to test the theory in the case of a rectangular plate in vacuum. The free vibrations of isotropic rectangular uniform plates were obtained for a variety of boundary conditions (Charbonneau & Lakis 1999). The computed natural frequencies were compared with other theories and with data from experiments.

Here, we present some example to test the theory in the case of a rectangular plate submerged in a fluid, floating on a fluid or supporting a fluid at rest.

3.8.1 Validation of model

By examining at the convergence criteria, it is easy to determine the advantage of this method, a combination of the finite element method and classical plate theory. A preliminary set of calculations has been made on a plate in vacuum to determine the rate of convergence of the method. We calculated the first six natural frequencies of a plate simply supported on its four edges and we varied the number of elements from 1 to 64. Figure 3.6 shows that with eight elements more than five frequencies have converged. The convergence is rapid since we are using a power series which closely represents the real displacement of a plate in bending.

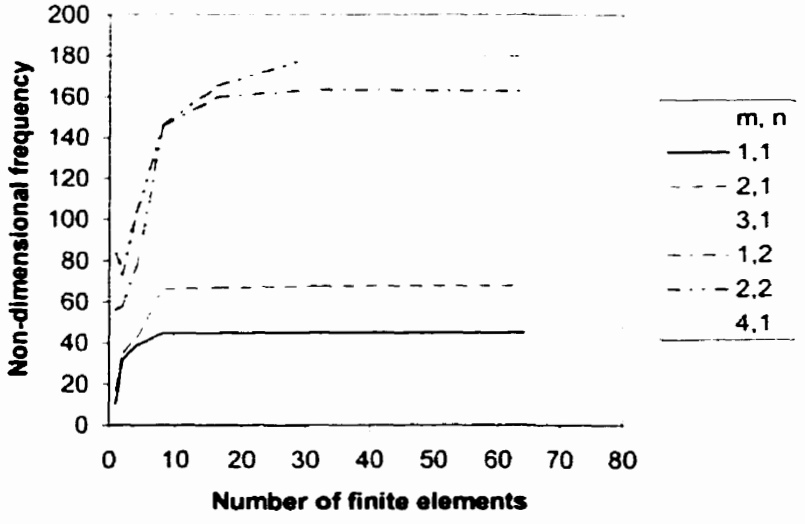

Fig. 3.6. Non-dimensional natural frequency, $\Omega = \omega a^2(\rho t/K)^{1/2}$, of a simply supported rectangular plates as a function of the number of finite elements for the first six modes.

Moreover, if we compare our method to classical theory, we can see that the error is small. Table 3.2 shows the relative error between our method and the exact solution for a plate being simply supported on two opposite edges. The error is less than 10% for four modes with only sixty-four (8 x 8) elements.

Table 3.2. Relative error between the exact solution of rectangular plate simply supported and a 64 finite element model.

M, N	1, 1	2, 1	3, 1	1, 2	2, 2	4, 1
Exact solution : f (Hz)	83.50	133.61	217.12	283.9	334.0	334.0
Our method : f (Hz)	76.16	114.69	191.27	275.44	303.94	305.19
% error	8.79	14.16	11.91	2.98	9.00	8.63

In order to prove the theory developed in this paper, a number of calculations have been performed for different cases corresponding to published experimental and numerical results.

The first comparison involves the work of Haddara & Cao (1996). They conducted experiments on rectangular steel plates submerged in water with the following geometry: length of 655.0 mm, a width of 201.65 mm and a thickness of 9.36 mm. For the measurements in water, the plates are placed in a tank 1300.0 mm long, 550.0 mm wide and 800.0 mm deep. Two different boundary conditions were analyzed: clamped at the two shortest sides with the other edges free (CFCF) and simply supported on the two shortest side while the other edges remain free (SFSF). The result of these experiments for the first three bending modes are presented in table 3.3 against the theory developed by Haddara & Cao and against the combination of the finite element method and classical plate theory developed in this paper. The results obtained by the present method agree with both experimental and analytical results predicted by Haddara & Cao. We can also see that the boundary conditions have little or no impact on the drop in natural frequencies.

Table 3.3. Comparison between the natural frequencies obtained by the present method and the natural frequencies obtained experimentally and analytically by Haddara and Cao (1996) for a rectangular plate submerged in water.

BOUNDARY CONDITIONS	MODE NO.	PRESENT METHOD NATURAL FREQ. (HZ)		HADDARA AND CAO (IN WATER ONLY) NATURAL FREQ. (HZ)		% OF CHANGE DUE TO BOUNDARY CONDITIONS
		Vacuum	Water	Experimental	Analytical	
CFCF	1	117.8	72.1	57.44	67.63	35
	2	324.1	198.3	167.01	198.6	
	3	636.5	389.6	345.0	414.7	
SFSF	1	50.9	31.1	28.72	28.34	36
	2	204.2	125.0	117.13	120.94	
	3	461.8	282.6	281.80	291.84	

The second comparison will take into consideration the analysis done by Joseph & al. (1990) which gives results from a finite element analysis of a rectangular plates submerged in water. Since there are no experimental values to compare with their results, we will use the work of Linholm et al. (1965) which presents an extensive table of resonant frequencies for cantilever plate in air or submerged in water. The plate under analysis here is a square steel plate of 200 mm x 200 mm with a thickness of 2.5 mm. The experiments were performed in a 1.83 m x 3.66 m x 2.44 m deep water tank with the cantilever plates being clamped to a rigid I-beam support structure. Table 3.4 shows the results computed for the two first bending modes by our method and by Joseph et al. (1990) and are compared with the experimental results from Lindholm et

al. (1969). The results shown in table 3.4 are in good agreement with both the experiments and the numerical results of the two other authors.

Table 3.4. Comparison between the present method and the finite element method proposed by Joseph at al. (1990), on one hand, and by the natural frequencies obtained experimentally by Lindholm (1969), on the other hand, for a cantilever square plate submerged in water.

	PRESENT METHOD		JOSEPH ET AL.		LINDHOLM	
	vacuum	water	vacuum	water	air	water
f_1 (Hz)	54.1	22.9	52.63	23.71	52.9	23.3
f_2 (Hz)	324.5	137.0	323.20	172.31	326	158

3.8.2 Influence of a fluid on a rectangular plate

Now that our method has been shown to give a good result, we can study the influence of a fluid surrounding a rectangular plate on its natural frequencies. Furthermore, the cases analyzed in the last section allow us to conclude that the decrease in the natural frequencies of a plate deeply submerged in fluid is principally dependant on the plate geometry. In order to quantify what is deeply submerged, the plates used in the previous examples will be analyzed with varying quantities of fluid above and under the plates.

We will first study the effect of varying the fluid height over the plate (h_1) on the plate first fundamental frequency. Figure 3.7 shows the influence of the fluid height for

two cantilever plates having a length to width ratio of 3.25 and 1.0. From this analysis, it can be stated that the influence of the fluid height on the natural frequency becomes constant when we have a fluid height equals to 40% or higher of the plate's length. Moreover, the longer is the plate, the less fluid is needed to lower the natural frequencies to constant values.

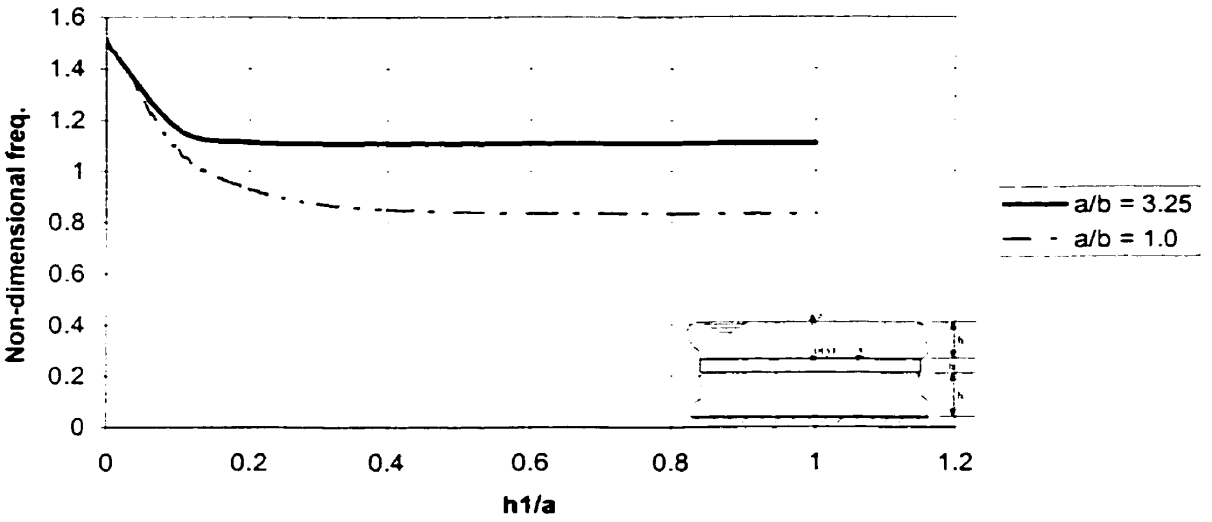

Fig. 3.7. Variation of non-dimensional first natural frequency, $\Omega = \omega a^2 (\rho t/K)^{1/2}$, of two cantilever plates as a function of the fluid height h_1.

By, analyzing the effect of the fluid under the plate (h_2), we can see from figure 3.8 that the natural frequency is no longer affected by the fluid once its depth under the plate is about 40% or more of the plate's length. Moreover, when we have a thin layer of fluid between the plate and the rigid bottom of the tank, we notice that the plate's natural frequency tends to zero. This result confirms what Moody (1995) has reported.

He found that the added mass factor tends to infinity when the fluid space between a vibrating and a rigid surface tends to zero. Indeed, if there is no fluid beneath the plate, the plate is resting on a rigid wall and consequently the rigid body motion of the plate has a natural frequency tending to zero. The virtual mass may be of small significance if the structural mass is relatively large. However, in our case, we are dealing with thin plates that means, which the fluid mass matrix becomes more important compared to the plate mass matrix and will significantly lower the natural frequencies.

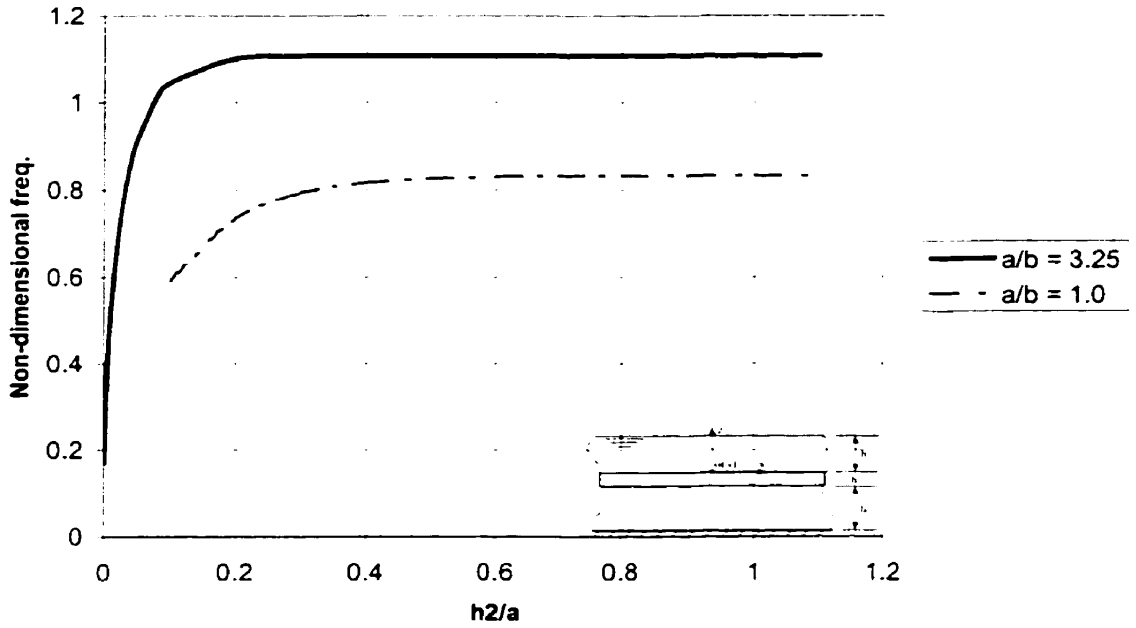

Fig. 3.8. Variation of non-dimensional first natural frequency, $\Omega = \omega a^2 (\rho t/K)^{1/2}$, of two cantilever plates as a function of the fluid depth h_2.

Finally, we looked at the contribution of the fluid over the plate compared to that of the fluid under the plate. Figure 3.9 shows that when we have more than 30% of the

plate's length of fluid both over and under the plate, the contributions of the two fluids are equal (assuming the quantity of fluid is the same on both sides). When we have less than 30% of the plate's length, the contributions of the two fluids are different. This is partially explained by the conclusion obtained from Figure 3.8. On the other hand, the fluid over the plate has its top surface free to oscillate. It is obvious that, when the fluid height tends to zero, the plate will vibrate at its natural frequencies in a vacuum.

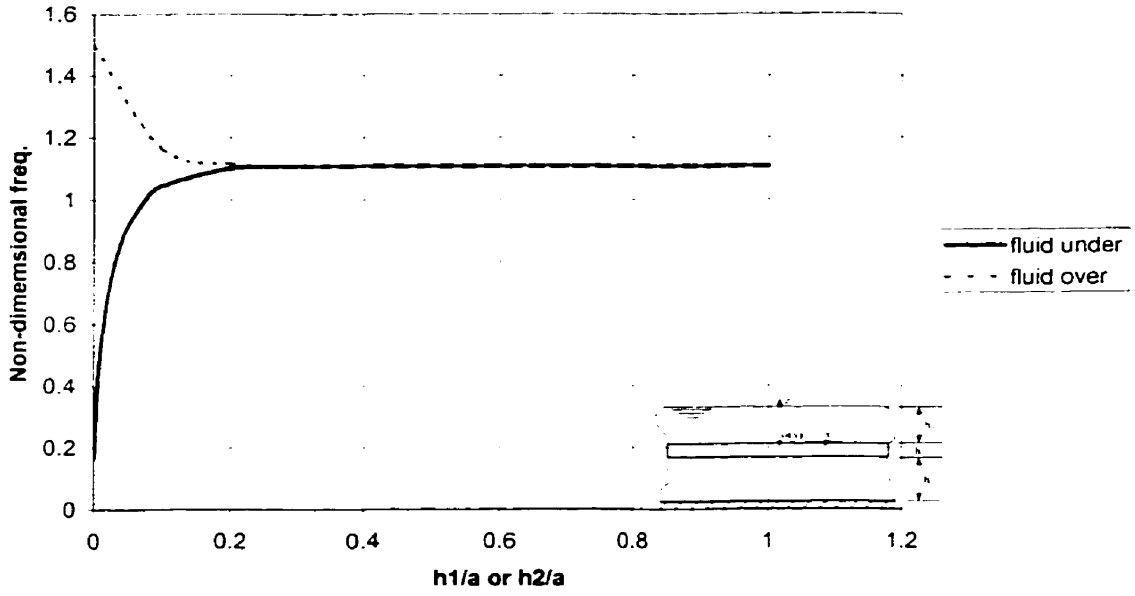

Fig. 3.9 Comparison of the fluid contribution over and under a cantilever plate on the first non-dimensional frequency, $\Omega = \omega\, a^2 (\rho t/K)^{1/2}$

3.9 CONCLUSION

The theory developed in this paper is used to predict the effect of the fluid inertia on the vibration characteristics of a thin isotropic rectangular plate totally submerged in a fluid, floating on a fluid or supporting a fluid.

A rectangular plate finite element was developed, making it possible to derive the displacement functions from the equation of motion of the plate. The mass and stiffness matrices of each element were obtained by exact analytical integration.

The fluid pressure was derived from the velocity potential taking into account the oscillation of the free surface, and from the linear impermeability and dynamic conditions applied to the plate-fluid interface. The finite element method was used to obtain the mass matrix of the fluid elements. The results obtained by this method were compared with other authors and satisfactory agreement was obtained. The dynamic characteristics were observed, and two effects on them of different boundary conditions and plate dimensions, as well as those of depths of submergence, were investigated.

Here we derived a polynomial which is, in fact, a power series expansion of the exact solution. This power series has proven to approximate more closely the exact solution of a plate in bending. In other studies made by our group on the shell domain (Lakis, A. A., Neagu, S. 1997, Selmane, A. & Lakis, A. A. 1997, Lakis, A. A. &

Païdoussis, M. P. 1971), it has been demonstrated that this theory gives as accurate results for low frequencies as for high frequencies. We are, therefore, able to analyze the response of excited plates submerged in fluid more accurately since we are using more modes and frequencies and that these frequencies are closer to those of the exact solution.

The next logical step would be the analysis of a fluid in motion over and under a plate. For this to be done, the fluid stiffness and damping matrices would have to be calculated.

3.10 REFERENCES

Amabili, M. 1996 Effect of finite fluid depth on the hydroelastic vibrations of circular and annular plates. *Journal of sound and vibration* **193**, 159-171.

Charbonneau , E. & Lakis, A. A. 1999 Semi-analytical shape functions in the finite element analysis of rectangular plates. *Rapport technique No EPM/RT-99/19*, École Polytechnique de Montréal.

Fu, Y. & Price, W. G. 1987 Interactions between a partially or totally immersed vibrating cantilever plate and the surrounding fluid. *Journal of Sound and Vibration* **118**, 495-513.

Haddara, M. R. & Cao, S. 1996 A study of the dynamic response of submerged rectangular flat plates. *Marine structures* **9**, 913-933.

Joseph, P., Muthuveerappan, G. & Ganesan, N. 1990 Vibrations of generally orthotropic plates in fluids. *Composite Structures* **15**, 25-42.

Lamb, H. 1921 On the vibration of an elastic plate in contact with water. *Proc. Royal Soc. London* **A 98**, 205-216.

Lakis, A. A. & Païdoussis, M. P. 1971 Free vibration of cylindrical shells partially filled with liquid. *Journal of Sound and Vibration* **19**, 1-15.

Lakis, A. A., Neagu, S. 1997 Free surface effects on the dynamics of cylindrical shells partially filled with liquid. *Journal of Sound and Vibration* **207**, 175-205.

Leissa, A. W. 1973 *Vibration of shells*, NASA, SP-288.

Lindholm, U. S. & al. 1965 Elastic vibration characteristics of cantilever plates in water. *Journal of Ship Research* June, 11-22.

Moody, F. J. 1995 Virtual mass for fluid space between rigid and vibrating surfaces. *Proc. of the ASME fluids Eng. div.* **234**, 25-27.

Robinson, N. J. & Palmer, S. C. 1990 A modal analysis of rectangular plate floating on an incompressible liquid. *Journal of Sound and Vibration* **142**, 453-460.

Selmane, A. & Lakis, A. A. 1997 Vibration analysis of anisotropic open cylindrical shells subjected to flowing fluid. *Journal of fluids and structures* **11**, 111-134.

Soedel, S. M. & Soedel W. 1994 On the free and forced vibration of a plate supporting a freely sloshing surface liquid. *Journal of Sound and Vibration* **171**, 159-171.

APPENDIX A: MATRIX [A]

The terms of matrix [A] are a defined as follows:

$$
\begin{bmatrix}
0 & 0 & 0 & 1 & 0 & 0 & 0 & 0 & 0 & 0 & 0 & 0 & 0 & 0 & 0 & 0 & 0 & 0 & 0 & 0 & 0 & 0 & 0 & 0 \\
0 & 0 & 0 & 0 & 0 & 0 & 0 & 1 & 0 & 0 & 0 & 0 & 0 & 0 & 0 & 0 & 0 & 0 & 0 & 0 & 0 & 0 & 0 & 0 \\
0 & 0 & 0 & 0 & 0 & 0 & 0 & 0 & 0 & 0 & 0 & 0 & 0 & 0 & 0 & 0 & 0 & 0 & 0 & 0 & 0 & 0 & 0 & 1 \\
0 & 0 & 0 & 0 & 0 & 0 & 0 & 0 & 0 & 0 & 0 & 0 & 0 & 0 & 0 & 0 & 0 & 0 & 0 & \frac{1}{a} & 0 & 0 & 0 & 0 \\
0 & 0 & 0 & 0 & 0 & 0 & 0 & 0 & 0 & 0 & 0 & 0 & 0 & 0 & 0 & 0 & 0 & 0 & 0 & 0 & 0 & 0 & \frac{1}{b} & 0 \\
0 & 0 & 0 & 0 & 0 & 0 & 0 & 0 & 0 & 0 & 0 & 0 & 0 & 0 & 0 & 0 & 0 & 0 & \frac{1}{a \cdot b} & 0 & 0 & 0 & 0 & 0 \\
0 & 1 & 0 & 1 & 0 & 0 & 0 & 0 & 0 & 0 & 0 & 0 & 0 & 0 & 0 & 0 & 0 & 0 & 0 & 0 & 0 & 0 & 0 & 0 \\
0 & 0 & 0 & 0 & 0 & 1 & 0 & 1 & 0 & 0 & 0 & 0 & 0 & 0 & 0 & 0 & 0 & 0 & 0 & 0 & 0 & 0 & 0 & 0 \\
0 & 0 & 0 & 0 & 0 & 0 & 0 & 0 & 0 & 0 & 0 & 1 & 0 & 0 & 0 & 1 & 0 & 0 & 0 & 1 & 0 & 0 & 0 & 1 \\
0 & 0 & 0 & 0 & 0 & 0 & 0 & 0 & 0 & 0 & 0 & \frac{3}{a} & 0 & 0 & 0 & \frac{2}{a} & 0 & 0 & 0 & \frac{1}{a} & 0 & 0 & 0 & 0 \\
0 & 0 & 0 & 0 & 0 & 0 & 0 & 0 & 0 & 0 & \frac{1}{b} & 0 & 0 & 0 & \frac{1}{b} & 0 & 0 & 0 & \frac{1}{b} & 0 & 0 & 0 & \frac{1}{b} & 0 \\
0 & 0 & 0 & 0 & 0 & 0 & 0 & 0 & 0 & 0 & \frac{3}{a \cdot b} & 0 & 0 & 0 & \frac{2}{a \cdot b} & 0 & 0 & 0 & \frac{1}{a \cdot b} & 0 & 0 & 0 & 0 & 0 \\
1 & 1 & 1 & 1 & 0 & 0 & 0 & 0 & 0 & 0 & 0 & 0 & 0 & 0 & 0 & 0 & 0 & 0 & 0 & 0 & 0 & 0 & 0 & 0 \\
0 & 0 & 0 & 0 & 1 & 1 & 1 & 1 & 0 & 0 & 0 & 0 & 0 & 0 & 0 & 0 & 0 & 0 & 0 & 0 & 0 & 0 & 0 & 0 \\
0 & 0 & 0 & 0 & 0 & 0 & 0 & 0 & 1 & 1 & 1 & 1 & 1 & 1 & 1 & 1 & 1 & 1 & 1 & 1 & 1 & 1 & 1 & 1 \\
0 & 0 & 0 & 0 & 0 & 0 & 0 & 0 & \frac{3}{a} & \frac{3}{a} & \frac{3}{a} & \frac{3}{a} & \frac{2}{a} & \frac{2}{a} & \frac{2}{a} & \frac{2}{a} & \frac{1}{a} & \frac{1}{a} & \frac{1}{a} & \frac{1}{a} & 0 & 0 & 0 & 0 \\
0 & 0 & 0 & 0 & 0 & 0 & 0 & 0 & \frac{3}{b} & \frac{2}{b} & \frac{1}{b} & 0 & \frac{3}{b} & \frac{2}{b} & \frac{1}{b} & 0 & \frac{3}{b} & \frac{2}{b} & \frac{3}{b} & 0 & \frac{3}{b} & \frac{2}{b} & \frac{1}{b} & 0 \\
0 & 0 & 0 & 0 & 0 & 0 & 0 & 0 & \frac{9}{a \cdot b} & \frac{6}{a \cdot b} & \frac{3}{a \cdot b} & 0 & \frac{6}{a \cdot b} & \frac{4}{a \cdot b} & \frac{2}{a \cdot b} & 0 & \frac{3}{a \cdot b} & \frac{2}{a \cdot b} & \frac{1}{a \cdot b} & 0 & 0 & 0 & 0 & 0 \\
0 & 0 & 1 & 1 & 0 & 0 & 0 & 0 & 0 & 0 & 0 & 0 & 0 & 0 & 0 & 0 & 0 & 0 & 0 & 0 & 0 & 0 & 0 & 0 \\
0 & 0 & 0 & 0 & 0 & 0 & 1 & 1 & 0 & 0 & 0 & 0 & 0 & 0 & 0 & 0 & 0 & 0 & 0 & 0 & 0 & 0 & 0 & 0 \\
0 & 0 & 0 & 0 & 0 & 0 & 0 & 0 & 0 & 0 & 0 & 0 & 0 & 0 & 0 & 0 & 0 & 0 & 0 & 1 & 1 & 1 & 1 & 1 \\
0 & 0 & 0 & 0 & 0 & 0 & 0 & 0 & 0 & 0 & 0 & 0 & 0 & 0 & 0 & 0 & \frac{1}{a} & \frac{1}{a} & \frac{1}{a} & \frac{1}{a} & 0 & 0 & 0 & 0 \\
0 & 0 & 0 & 0 & 0 & 0 & 0 & 0 & 0 & 0 & 0 & 0 & 0 & 0 & 0 & 0 & 0 & 0 & 0 & 0 & \frac{3}{b} & \frac{2}{b} & \frac{1}{b} & 0 \\
0 & 0 & 0 & 0 & 0 & 0 & 0 & 0 & 0 & 0 & 0 & 0 & 0 & 0 & 0 & 0 & \frac{3}{a \cdot b} & \frac{2}{a \cdot b} & \frac{1}{a \cdot b} & 0 & 0 & 0 & 0 & 0
\end{bmatrix}
$$

APPENDIX B: NOMENCLATURE

a	length of a rectangular finite element
A	length of the rectangular plate
A_i	defined by equation (3.3) i = 0, 1, 2, 3
A_1	defined by equation (3.26)
A_2	defined by equation (3.26)
b	width of a rectangular finite element
B	width of a rectangular finite element
$B_{i,j}$	defined in equation (3.34)
B_j	defined by equation (3.3) i = 0, 1, 2, 3
C_1	defined by equation (3.27)
C_i	defined by equation (3.18)
D	membrane stiffness, $Et/(1-\nu^2)$
E	Young's modulus
h_1, h_2	fluid height and fluid depth
K	bending stiffness, $Et^3/12(1-\nu^2)$
N	number of finite elements
$P_{i,j}$	terms of the elasticity matrix, i =1, 2, ..., 6, j =1, 2, ..., 6
$S^{(u)}_{i,j}$, $S^{(v)}_{i,j}$, $S^{(w)}_{i,j}$	defined by equation (33), i = 1, 2, ..., 16 ; j = 1, 2, ..., 16
t	thickness of the rectangular plate
u_i, v_i, w_i	nodal displacements, i = 1, ..., 4

U, V, W	in-plane and normal displacement of a rectangular plate
x, y	length and width co-ordinate of the plate
$w_{i,x}, w_{i,y}, w_{i,xy}$	nodal rotations and twisting, $i = 1, \ldots, 4$
W_p	displacement function defined by equation (3.3)
Z	defined by equation (3.30)
δ_i	degree of freedom at node i, $i = 1, \ldots, 4$
$\varepsilon_x, \varepsilon_y, \varepsilon_{xy}$	deformations of the plate reference surface
$\kappa_x, \kappa_y, \kappa_{xy}$	changes in curvature and twisting of the plate reference surface
μ_λ	defined by equation (3.22)
$\Phi(x, y, t)$	fluid velocity potential
ρ	density of the plate material
ρ_f	density of the fluid
υ	Poisson's ratio
ω	angular natural frequency, rad s^{-1} in vacuum
ω_f	angular natural frequency, rad s^{-1} in fluid
Ω	non-dimensional frequency, $\omega a^2(\rho t/K)^{1/2}$
ψ	phase angle

List of matrices

[A]	defined by equation (3.7), given in Appendix A
[B]	defined by equation (3.10)

$\{C\}$	defined by equation (3.5)
$[C_f]$	damping matrix of the fluid
$[D]$	defined by equation (3.9)
$\{F\}$	external force vector
$[k_s]$	stiffness matrix of one plate element
$[K_s]$	stiffness matrix of the total plate
$[K_f]$	stiffness matrix of the total fluid
$[m_f]$	mass matrix of one fluid element
$[m_s]$	mass matrix of one plate element
$[M_s]$	mass matrix of the total plate
$[M_f]$	mass matrix of the fluid
$[N]$	defined by equation (3.8)
$[P]$	elasticity matrix
$[R]$	defined by equation (3.4)
$[S_f]$	defined by equation (3.33)
$\{\Delta\}$	displacement vector
$\{\varepsilon\}$	strain vector
$\{\sigma\}$	stress vector
$\{\delta_i\}$	degrees of freedom at node i
$\{\delta_T\}$	degrees of freedom for the total plate
$\{\delta_{0,T}\}$	Amplitude of the plate motion

CONCLUSION

L'objectif de cette recherche était de présenter une méthode de développement des fonctions de déplacement pour une plaque rectangulaire mince et, ensuite, utiliser ces fonctions de déplacement dans l'analyse d'un système couplé fluide-structure. Cette méthode permettra ainsi de prédire l'effet de l'inertie du fluide sur les caractéristiques vibratoires d'une plaque rectangulaire mince complètement submergé dans un fluide, flottant sur un fluide ou supportant celui-ci. Par conséquent, les fonctions de déplacement choisies devaient être compatibles autant avec la théorie classique des plaques minces qu'avec la solution de la pression du fluide à l'interface de la plaque.

Les fonctions de déplacements trouvées sont ensuite utilisées avec la théorie des éléments finis pour calculer les matrices de masse et de rigidité d'un élément de plaque rectangulaire à vingt-quatre degrés de liberté. La convergence de la méthode pour une plaque dans le vide a été vérifiée. De plus, les fréquences naturelles et mode propres pour différentes conditions frontières ont été calculés. Les résultats obtenus ont été comparés avec ceux d'autres auteurs et ont démontré la précision de la méthode. La qualité des résultats était prévisible puisque cette méthode combine l'avantage des éléments finis et la précision d'une formulation dérivée de la théorie des plaques minces.

L'étude de la convergence de la méthode pour une plaque simplement supportée sur tous les cotés nous a appris, contrairement à ce que l'on pourrait s'attendre, que l'élément semble sous estimer la rigidité de la plaque. Cependant, en analysant le nombre de degrés de liberté contenus dans un modèle avec peu d'éléments de la plaque en flexion, l'explication du phénomène est tout à fait simple. Lorsque la plaque est modélisée avec un seul élément et que tous les cotés sont simplement supportés, il ne reste que les degrés de liberté associés aux rotations de la plaques. Ceux-ci ne peuvent pas surestimer la rigidité de la plaque, car le degré donnant la rigidité en flexion est le déplacement normal à la plaque qui est absent lors de la modélisation de la plaque avec un seul élément. Pour prouver cette affirmation, l'annexe I présente la convergence de la même plaque, mais avec les conditions aux frontières suivantes : encastrée à une extrémité et tous les autres cotés libres. Cette plaque a donc après l'application des conditions aux frontières, même pour un modèle à un seul élément, des degrés de liberté associés aux déplacements normaux à la plaque ce qui lui confère une rigidité accrue.

Après avoir montré que l'élément de plaque représentait du mieux possible les déplacements d'une vraie plaque rectangulaire vibrante, nous pouvions attaquer le problème de la plaque en contact avec un fluide. Dans un premier temps, la pression du fluide a été dérivée à partir du potentiel de vitesse en tenant compte de l'oscillation de la surface libre et en appliquant les conditions dynamiques et d'imperméabilité à l'interface plaque-fluide. Cette démarche nous a permis permet d'obtenir une expression de la pression du fluide en fonction des déplacements nodaux de l'élément de

plaque. Utilisant la méthode des éléments finis, la matrice de masse de l'élément de fluide a été dérivée.

Grâce à cet élément de fluide, nous avons pu comparer les fréquences naturelles et modes propres de différentes plaques submergées dans un fluide avec ceux calculés par d'autres théories. Notre méthode donne des résultats qui concordent parfaitement avec ceux des autres auteurs. Par contre, notre méthode se différencie des autres par les points suivants : a) convergence rapide avec un nombre peu élevé d'éléments, b) possibilité de calculer les hautes fréquences avec précision et, c) élimine le besoin de nœuds supplémentaires pour les éléments de fluide ce qui réduit le temps de calcul.

En développant cette méthode, nous pouvions étudier l'effet de différentes conditions aux frontières, des dimensions de la plaque et de la profondeur du fluide sur les fréquences naturelles d'une plaque rectangulaire mince. Nous avons prouvé que les fréquences naturelles d'un système couplé fluide-structure ne dépendent pas de ses modes propres et très peu des conditions aux frontières, mais seulement de sa géométrie et des propriétés du fluide lorsque sa première fréquence naturelle est supérieure à 10 Hz. De plus, il a été démontré que l'effet du fluide sur la baisse des fréquences naturelles de la plaque devient constant lorsque le fluide atteint une hauteur ou une profondeur égale à 40% de la longueur de la plaque. Par contre, lorsque la plaque repose sur une couche mince de fluide, c'est à dire que la profondeur du fluide est moins

de 10% de la longueur de la plaque, les fréquences naturelles de celle-ci diminuent drastiquement et tendent vers zéro.

Dans ce mémoire, nous avons dérivé un polynôme qui est, en réalité, un développement en série de puissance de la solution homogène exacte de l'équation différentielle bi-harmonique d'une plaque rectangulaire mince. Cette solution tend à estimer plus exactement la solution d'une plaque en flexion. Dans d'autres études faites par notre groupe de recherche dans le domaine des coques (Lakis et Neagu (1997), Selmane et Lakis (1997), Lakis, Sami, et Rousellet, (1978)), il a été démontré que cette théorie donne des résultats aussi précis pour les basses que les hautes fréquences. Cela permet d'analyser la réponse des plaques submergées soumises à des excitations extérieures plus précisément puisque nous utilisons un plus grand nombre de fréquences et de modes propres dans le calcul de la réponse et que ces fréquences et modes sont plus près de la solution exacte.

Pour rendre ces travaux plus intéressant pour l'industrie, un élément de plaque mince quadrilatéral devrait être dérivé. Du coté du système fluide-structure, la prochaine étape serait de dériver une matrice de rigidité et d'amortissement pour l'élément de fluide dans le cas d'un fluide en écoulement sur la plaque.

BIBLIOGRAPHIE

Amabili, M. (1996). Effect of finite fluid depth on the hydroelastic vibrations of circular and annular plates. Journal of sound and vibration, **193**, 159-171.

Bogner, F. K. & al. (1967). A cylindrical shell element. AIAA Journal., **5**, 745-750.

Bogner, F. K. & al. (1966). The generation of interelement-compatible stiffness and mass matrices by the use of interpolation formulas. Proceeding of the Conference on Matrix Method in Structural Mechanics, Wright-Patterson Air Force Base/Air Force flight Dynamics Lab. TR-66-80.

Charbonneau , E. & Lakis, A. A. (1999). Semi-analytical shape functions in the finite element analysis of rectangular plates. Rapport technique No EPM/RT-99/19, École Polytechnique de Montréal.

Fu, Y. & Price, W. G. (1987). Interactions between a partially or totally immersed vibrating cantilever plate and the surrounding fluid. Journal of Sound and Vibration, **118**, 495-513.

Grinsted, B. (1952). Nodal Pattern Analysis. Proc. Inst. Mech. Eng., ser. A, **166**, pp.309-326.

Haddara, M. R. & Cao, S. (1996). A study of the dynamic response of submerged rectangular flat plates. Marine structures, **9**, 913-933.

Joseph, P., Muthuveerappan, G. & Ganesan, N. (1990). Vibrations of generally orthotropic plates in fluids. Composite Structures, **15**, 25-42.

Lakis, A. A. (1976). Theoretical model of cylindrical structures containing turbulent flowing fluids. 2nd Int. Symp. on Finite Element Methods in Flow Problems, Santa margherita Ligure, Italy.

Lakis, A.A. & Laveau, A. (1991). Non-linear dynamic analysis of anisotropic cylindrical shells containing a flowing fluid. Int. J. solids struct., **28**, 1079-1094.

Lakis, A. A., Neagu, S. (1997). Free surface effects on the dynamics of cylindrical shells partially filled with liquid. Journal of Sound and Vibration, **207**, 175-205.

Lakis, A. A. & Païdoussis, M. P. (1971). Free vibration of cylindrical shells partially filled with liquid. Journal of Sound and Vibration, **19**, 1-15.

Lakis, A. A. & Paidoussis, M. P. (1972). Dynamic analysis of axially non-uniform thin cylindrical shells. J. Mech. Eng. Sci., **14**, 49-71.

Lakis, A.A. & Paidoussis, M.P. (1971). Free vibration of cylindrical shells partially filled with liquid. Journal of Sound and Vibration, **19**, 1-15.

Lakis, A. A. & Paidoussis, M. P. (1972). Prediction or the response of a cylindrical shell to arbitrary of boundary-layer-induced random pressure field. Journal of Sound and Vibration, **25**, 1-27 .

Lakis, A. A. & Paidoussis, M. P. (1973). Shell natural frequencies of the pickering steam generator. Anatomic Energy of Canada Ltd., AECL Report No. 4362.

Lakis, A. A., Sami, S. M. & Rousellet, J. (1978). Turbulent two phases flow loop facility for predicting wall-pressure fluctuation and shell response. 24th Int. Instrument Symp. Albuquerque, New Mexico.

Lakis, A. A. & Sinno, M. (1992). Free vibration of axisymmetric and beam-like cylindrical shells partially filled with liquid. Int. j. numer. methods eng., **33**, 235-268.

Lakis, A.A., Tuy, N., Laveau, A. & Selmane, A. (1989). Analysis of axially non-uniform thin spherical shells. Int. Symp. STRUCOPT-COMPUMAT, Paris, France, pp. 80-85.

Lakis, A. A., Van Dyke, P. & Ouriche, H. (1992). Dynamic analysis of anisotroppic fluid-filled conical shells. J. Fluids Struct., **6**, 135-162.

Lamb, H. (1921). On the vibration of an elastic plate in contact with water. Proc. Royal Soc. London, **A 98**, 205-216.

Leissa, A. W. (1973). Vibration of shells, NASA, SP-288.

Leissa, A. W. (1969). Vibration of Plates, NASA, SP-160, 1969.

Lindholm, U. S. & al. (1965 June). Elastic vibration characteristics of cantilever plates in water. Journal of Ship Research, 11-22.

Love, A. E. H. (1944). A treatise on the Mathematical Theory of Elasticity, Dover, New York.

Martin, A.I. (1956). On the Vibration of Cantilever Plate. Quart. J. Mech. Appl. Math., **9**, pt 1, pp. 94-102.

Moody, F. J. (1995). Virtual mass for fluid space between rigid and vibrating surfaces. Proc. of the ASME fluids Eng. div., **234**, 25-27.

Robinson, N. J. & Palmer, S. C. (1990). A modal analysis of rectangular plate floating on an incompressible liquid. Journal of Sound and Vibration, **142**, 453-460.

Sanders, J. L. (1959). An improved first approximation theory for thin shell. NASA TR-24.

Selmane, A. & Lakis, A. A. (1997). Vibration analysis of anisotropic open cylindrical shells subjected to flowing fluid. Journal of fluids and structures, **11**, 111-134.

Soedel, S. M. & Soedel W. (1994). On the free and forced vibration of a plate supporting a freely sloshing surface liquid. Journal of Sound and Vibration, **171**, 159-171.

Szelard, R. (1974). Theory and Analysis of plate, Prenctice-Hall, Englewood Cliffs, NJ.

Turner, M. J. & al. (1956). Stiffness and Deflection Analysis of Complex Structure. J. Aero Sci., **23**, 805-823.

Zienkiewicz, O. C. (1977). The finite element method, 3rd edn., Mc Graw Hill, New York, 1977.

ANNEXE I: CONVERGENCE DE LA MÉTHODE

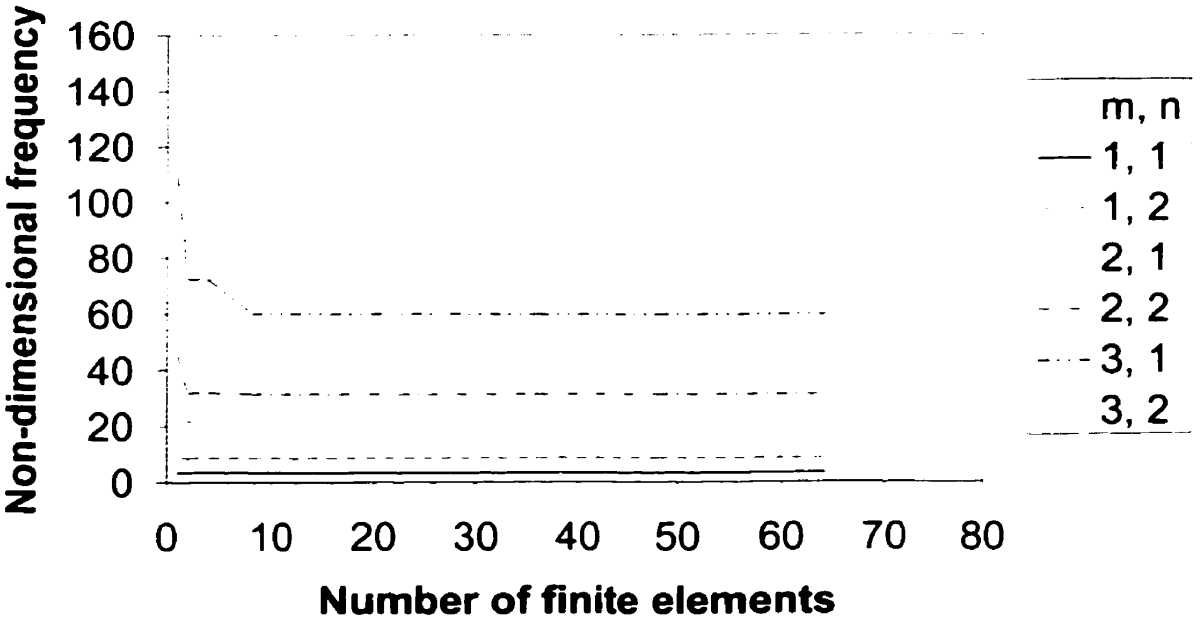

Convergence de la méthode pour la même plaque rectangulaire qu'à la figure 2.5, mais encastrée à une seule extrémité.